

**Development, Optimization and Dynamic testing of an adoptive MRE
based Base Isolated System Incorporating Nano and Micro Iron Particles**



By

Usman Tanveer Khan

(Registration No: Fall 2019-MS Structural Engg 00000319353)

Department of CIVIL Engineering

NUST Institute of Civil Engineering

School of CIVIL and Environmental Engineering

National University of Sciences & Technology (NUST)

Islamabad, Pakistan

(2023)

**Development, Optimization and Dynamic testing of an adoptive
MRE based Base Isolated System Incorporating Nano and Micro
Iron Particles**



By

Usman Tanveer Khan

(Registration No: Fall 2019-MS Structural Engg 00000319353)

A thesis submitted to National University of Sciences and Technology, Islamabad

In partial fulfillment of the requirements for the degree of

Master of Science in

Structural Engineering

Thesis Supervisor: Dr. M. Usman

NUST institute of Civil Engineering

School of Civil and Environmental Engineering

National University of Sciences and Technology (NUST)

Islamabad, Pakistan

THESIS ACCEPTANCE CERTIFICATE

Certified that final copy of MS Thesis written by Mr./Ms. Usman Tanveer Khan (Registration No: Fall 2019-MS Structural Engg 00000319353), NICE (School, College, Institute) has been vetted by undersigned, found complete in all respects as per NUST Status/Regulations/MS policy, is free from plagiarism, errors and mistakes and is accepted as partial fulfilment for award of MS degree. It is further certified that necessary amendments as point out by GEC members and foreign/local evaluators of the scholar have also been incorporated in the said thesis.

Signature: _____

Name of Supervisor _____

Date: _____

Signature (HOD, Structural Engineering) _____

NUST Institute of Civil Engineering
School of Civil & Environmental Engineering
National University of Sciences and Technology

Date: _____

Signature (Associate Dean): _____

Date: _____

Signature (Dean/Principal) _____

Date: 30 AUG 2023

PROF DR MUHAMMAD IRFAN
Principal & Dean
SCEE, NUST

Certificate of Approval

This is to certify that research work presented in this thesis entitled "Development, Optimization and Dynamic testing of an adoptive MRE based Base Isolated System Incorporating Nano and Micro Iron Particles" was conducted by Mr./Ms. Usman Tanveer Khan under the supervision of Dr. M. Usman.

No part of this thesis has been submitted else for any other degree. This thesis is submitted to the NUST Institute of Civil Engineering in partial fulfilment of the requirement for the degree of Master of Science in field of Structural Engineering.

Student Name: Usman Tanveer Khan

Examination Committee:

- a) GEC member 1: Dr. Hasan Farooq
.....
- b) GEC member 2: Dr. Azam Khan
Associate Professor
SCEE (NLCE)
- c) GEC member 3: Dr. Junaid Ahmad
Assistant Professor SCEE (NLCE)

Supervisor Name: Dr. M. Usman

Name of HOD: Dr. M. Usman


Name of Associate Dean:

Name of Principal & Dean:

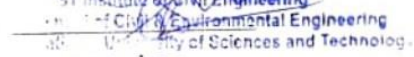
Signature: 

Signature: 

Signature: 

Signature: 

Signature: 
HoD Structural Engineering

Signature: 
NUST Institute of Civil Engineering
Department of Civil & Environmental Engineering
University of Sciences and Technology

Signature: 

Signature: 

PROF DR MUHAMMAD IRFAN
Principal & Dean
SCEE, NUST

Author's Declaration

I Usman Tanveer Khan hereby states that my MS thesis titled "Development, Optimization and Dynamic testing of an adoptive MRE based Base Isolated System Incorporating Nano and Micro Iron Particles" is my own work and has not been submitted previously by me for taking any degree from this university National University of Sciences and Technology, Islamabad or anywhere else in the country.

At any time if my statement is found to be incorrect even after I graduate, the university has the right to withdraw my MS degree.

Name of Student: Usman Tanveer Khan

Date: _____



Plagiarism Undertaking

I solemnly declare that the research work presented in the thesis titled "Development, Optimization and Dynamic testing of an adoptive MRE based Base Isolated System Incorporating Nano and Micro Iron Particles" is solely my research work with no significant contribution from any other person. Small contribution/help wherever taken has been duly acknowledged and that complete thesis has been written by me.

I understand the zero-tolerance policy of the HEC and National University of Sciences and Technology towards plagiarism. Therefore, I as an author of the above titled thesis declare that no portion of my thesis has been plagiarized and any material used as a reference is properly referred/cited.

I undertake that if I am found guilty of any formal plagiarism in the above titled thesis even after award of my MS degree, the university reserves the rights to withdraw/revoke my MS degree and that HEC and the university has the right to publish my name on the HEC/University website on which names of student are placed who submitted plagiarized thesis.

Student/Author Signature: _____



Name: Usman Tanveer Khan

Acknowledgement

I begin by expressing my profound gratitude to Allah Almighty for granting me the strength, wisdom, and guidance throughout this research journey.

I extend my heartfelt appreciation to my supervisor, Dr. M. Usman, the Head of Structural Engineering at NICE, Islamabad. His unwavering guidance, motivation, and compassion have been invaluable to me. Despite his demanding schedule, he consistently dedicated time for insightful discussions and provided invaluable support to his research students.

My sincere thanks go to the esteemed members of my Graduate Examination Committee, namely Dr. Hasan Farooq, Dr. Azam Khan, and Dr. Junaid Ahmad. Their constructive suggestions and assistance were instrumental in shaping the course of my research.

Given the interdisciplinary nature of my research, I had the privilege of working in three different laboratories: the Structural Lab at NICE, the Electronics Lab at SEECS, and the Dynamics Lab at MCE Risalpur. I wish to convey my deep appreciation to the lab engineers and technicians who displayed exceptional professionalism and support. Special recognition goes to Engr. Huzaifa, the lab engineer at MCE Risalpur, for his indispensable assistance.

I am indebted to my friends who willingly offered their assistance whenever needed, contributing significantly to the completion of my project. I want to specifically mention Engr. Hassaan Saleem for his unwavering support and invaluable insights during this process.

I am grateful to my employer, Engr. Amir Ghouri, for his support and cooperation in completing my project.

Lastly, I extend my heartfelt acknowledgment to my parents and siblings. Their unwavering motivation and encouragement provided me with the strength to persevere through this endeavor. Their belief in me was a constant source of inspiration.

Abstract

Seismic isolation is a widely employed technique on a global scale, aimed at prolonging the natural frequency of a structure and effectively isolating it from seismic disturbances. The proposed methodology entails the implementation of a flexible layer underneath a designed structure with the aim of mitigating the impact of seismic forces and minimizing structural displacements. The susceptibility of a base isolator to several seismic events mostly stems from its increased base drift. Large stiffness has the potential to mitigate base drift. However, it is important to note that this adjustment may result in the earthquake being shifted to a fixed system, so compromising certain fundamental benefits associated with the base isolator. This necessitates the utilization of an isolator that possesses the capability to adjust its stiffness. The implementation of such a base isolator would offer the requisite level of stiffness to mitigate the displacement of the base, while simultaneously preserving the effectiveness of response reduction measures. The objective of this work is to fabricate a laminated base isolator that has a significant capacity for carrying vertical loads. Nano and micro particles were integrated at a concentration of 40 percent. FEMM analysis yields the optimum dimensions of the isolator in order to determine the maximum flux. Subsequently, shake table testing was conducted to validate the observed correlation between the rise in magnetic flux of the base isolator and the corresponding increase in stiffness. The time period, frequency, and mode shapes of fixed and isolated systems were determined using MATLAB. The numerical analysis proved the effectiveness of the isolator in reducing lateral movement and minimizing story drift. Subsequently, dynamic testing was conducted at frequencies of 0.5Hz, 1Hz, and 1.5Hz, with amplitudes of 5mm, 10mm, and 15mm. Linear Variable Differential Transformers (LVDTs) were employed to measure the displacement of individual stories and isolators. This was done at different combinations of frequency and amplitude, while varying the current levels within the range of 0 to 4 amperes. The attainment of sufficient response reduction was observed while employing optimal current levels across various combinations of frequencies and amplitudes. The study additionally emphasizes the influence of amplitude and frequency of lateral loading on the dynamic response of a system equipped with a base isolator that possesses varying stiffness properties.

Key Words: MODF, Seismic Isolation, MRE base isolator, Smart Materials, Nano and Micro Iron Particles, Elastomers, Shake table, Sinusoidal Excitations

Table of Contents

Acknowledgement	vii
Abstract.....	viii
List of Figures	xi
List of Tables	xiii
Chapter 1: Introduction.....	1
1.1 Base Isolation	2
1.2 MRE in Base Isolator	3
1.3 Fundamentals of Base Isolation	4
1.4 Problem Statement	4
1.5 Research Objectives	5
1.6 Scope of Research	5
1.7 Thesis Organization.....	5
Chapter 2: Literature Review.....	6
2.1 Types of Base Isolators	6
2.2 Principle of Base Isolator	8
2.3 Smart Materials	9
2.4 Base Isolator limitations, and technological advancements in seismic mitigation ...	10
2.5 Advancement in MRE.....	12
Chapter 3: Methodology and Material.....	16
3.1 Elastomer Size.....	18
3.2 Optimized Sized of Elastomers	19
3.3 Electromagnetic Coil.....	21
3.4 Steel Components.....	23
3.4.1 Top Plate	23
3.4.2 Bottom Plate.....	23

3.4.3	Steel Yoke.....	24
3.4.4	Steel Lamination	25
3.5	Elastomers	25
3.6	Silicon Rubber.....	26
3.7	Iron Particles	27
3.8	DC Supply	28
3.9	Stiffness Calculation	29
3.10	Mode Shapes	30
3.11	Frame.....	32
Chapter 4: Results and Discussion		35
4.1	Experimental Setup	35
4.2	Effect of Amplitude.....	36
4.3	Effect of Frequency	37
4.4	Base Drift	39
4.5	Acceleration Response	41
Chapter 5: Conclusion		45
References.....		46

List of Figures

Figure 1: Tectonic map of South Asia	1
Figure 2: Behavior comparison of Fixed base and Isolated Base System	3
Figure 3: Examples of Base Isolated buildings (a) Daxing International Airport, China (b) Court of Appeals, California, USA.....	4
Figure 4:(a) Typical schematics of Lead Rubber Bearing (b) Typical schematics of Sliding Bearing.....	6
Figure 5: Comparison of Single-Layer and Multi-layer Elastomeric Bearing	7
Figure 6: Base displacement and Base acceleration comparison of Base Isolator having (a) High Damping Rubber (b) Low damping rubber.	8
Figure 7: Effect of Variable frequency range of Active isolated structure on spectral acceleration	9
Figure 8: Magnetizable particles in MR system (a) without magnetic flux (b) with magnetic flux	13
Figure 9: Simplified MDOF representation of the models studied (a) Fixed Base system (b) Isolated Base system.	16
Figure 10: Arrangement fabricated for the calibration of Load Cell.....	17
Figure 11: Loading Time Histories applied for different cases (a) 0.5 Hz, 5mm (b) 0.5 Hz, 10mm (c) 0.5 Hz, 15mm (d) 1Hz, 5mm (e) 1Hz 10mm (f) 1Hz, 15mm (g) 1.5 Hz, 5mm (h) 1.5Hz, 10mm (i) 1.5Hz, 15mm.....	18
Figure 12: Overlapping Area (A) of the top and bottom plates of the isolation bearing in fully deformed state.....	19
Figure 13: Finite Element Method Magnetics (FEMM) model for optimizing sizes of various steel components for maximum magnetic flux.....	20
Figure 14: Magnetic flux contours obtained from FEMM for optimized size of steel components.	20
Figure 15: Variation of magnetic flux along (a) Horizontal Axis (b) Vertical Axis	21
Figure 16: Electromagnetic Coil for providing magnetic flux to whole assembly.....	22
Figure 17: Magnetic Flux variation with Current.....	22
Figure 18: (a) Top Plate used in fixing Base Isolator to Steel Frame (b) Bottom Plate used in fixing Base Isolator to Shake Table	23
Figure 19: Steel Yoke employed for enclosing whole assembly.	24
Figure 20: Laminated Base Isolator with alternating elastomeric and steel layers.....	25

Figure 21: Silicon Rubber (Part A and Part B) and Silicon Oil.....	26
Figure 22: (a) Micro Sized Iron Particles (b) Nano Sized Iron Particles.....	27
Figure 23: 3-D printed mould for casting elastomer layers.	28
Figure 24: (a) Casting and curing of MRE layers (b) Sonification for homogeneous mixture of MRE.....	28
Figure 25: Direct Current (DC) Variation with Voltage having electromagnetic coil as resistance.....	29
Figure 26: Experimental Setup for Stiffness Calculation	29
Figure 27: Components of Load Cell arrangement.....	30
Figure 28: Mode Shapes of Fixed-base (Blue) and MRE isolated systems (others) at various current values	31
Figure 29: (a) Modified Steel Frame on Shake table (b) DC Supply for providing required values of current.....	33
Figure 30: Experimental Setup for Dynamic Testing at various sinusoidal excitations.....	35
Figure 31: Effect of current in displacement reduction (a)5 mm 1Hz (b)5 mm 1.5Hz	36
Figure 32: Effect of current in displacement reduction (a)10 mm 1Hz (b) 10 mm 1.5Hz	37
Figure 33: : Effect of current in displacement reduction (a)15mm 1Hz (b)15mm 1.5Hz	37
Figure 34: Effect of frequency in response reduction in (a) Story 1 (b) Story 2 (c) Story 3 ...	39
Figure 35: Base Drift reduction for (a) 5mm (b) 10mm (c) 15mm	40
Figure 36: Acceleration response for (a) 5mm 0.5Hz (b) 5mm 1.5Hz (a) 10mm 0.5Hz (a) 10mm 0.5Hz (a) 15mm 0.5Hz (a) for 15mm 0.5Hz	42
Figure 37: Story Drift reduction (a) 5mm (b) 10mm (c) 15mm	43

List of Tables

Table 1: Optimized Components of Base Isolator assembly	21
Table 2: Optimized Electromagnetic Coil dimensions	22
Table 3: Optimize Mix proportion of elastomer for maximum magnetic flux.....	25
Table 4: Properties of Silicon Rubber used in elastomer.....	26
Table 5: Chemical Composition and Physical Properties Comparison	27
Table 6: Frequency of Fixed base and Isolated System at various current values	31
Table 7: Time Period of Fixed base and Isolated System at various current values	32
Table 8: Initial and Modified frame properties after addition of stiffening components	33
Table 9: Parameters for different test cases	36
Table 10: Optimized Current Values for response reduction	44

Chapter 1: Introduction

Earthquakes are responsible for too much destruction to human life and property. Due to their nature, it is extremely difficult to accurately predict their occurrence. Sometimes they are accompanied by Tsunamis or volcanic eruptions and can easily overwhelm the Disaster Management efforts of humans [1]. They are not restricted to a confined area, but a large part of human settlement lives under the constant threat of these earthquakes. Many of these earthquakes occur at plate boundaries [2]. Ring of fire in Pacific Ocean and Japan where 4 of these tectonic plates coincide saw many destructive earthquakes in the past, for example Kobe earthquake. Pakistan too is vulnerable to such threat. Indian plate and Eurasian plate meet each other in Pakistan cutting the whole country in half as shown in figure 1. Kashmir earthquake, an earthquake of 7.1 magnitude in 2005 shook the region resulting in the death of 80000 people and an estimated displacement of 4 million while the Economic loss to Pakistan was 2.6 percent of its GDP according to World Bank [3]. The reports also mention the absence of earthquake resistant systems or techniques in buildings in high seismic zones. The dynamic response of a structure depends upon the type of earthquake, its intensity as well as its source and the designer must consider these effects in design [4-6]. The buildings having vertical deformity such as weak story, inadequate detailing is prone to earthquake forces.

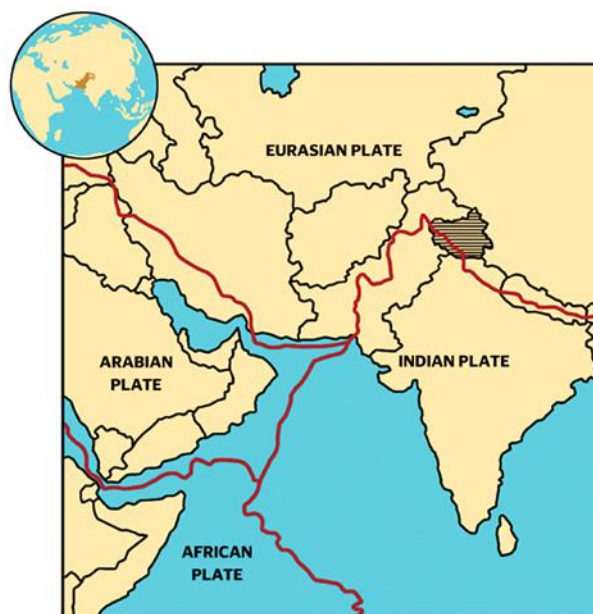


Figure 1: Tectonic map of South Asia

Earthquake mitigation techniques have seen many improvements in the past centuries. The first technique was making the structure bulky to mitigate the displacement, but it has some serious

drawbacks as a heavier structure increases the acceleration demands of the structure and attract the earthquake forces to its structural as well as non-structural components. This technique is very inefficient, impractical, and costly. Dampers are a very attractive choice for creating an earthquake resilient structure. Supplementary dampers are added to dissipate the earthquake energy and to keep the structural integrity of the system [7]. Spring mass damper: tuned mass dampers; Viscous dampers have shown good performance against earthquakes [8]. Lead rubber bearing has the advantage of combining damping, flexibility at lateral loads and stiffness and service load into a single compact unit [9]. The use of high damping may reduce the structural displacement in long period earthquakes however it increases the acceleration demands in short period earthquakes leading to a higher risk of damaging to non-structural components .

Conventional system may not be suitable for some structures such as Hospitals and Fire brigade offices which need to be always operational especially at a time of natural disasters [10]. Increasing the size of structure or introducing different types of dampers may reduce the displacement of the system, however they also tend to increase the forces and attract the earthquake towards themselves. In addition, these methods are expensive, need constant maintenance and may or may not work against variable earthquakes due to their passive nature. So, there was a need to introduce a system which can isolate the superstructure from the ground motions. A seismic isolation system may be used to decouple the structure [11, 12].

1.1 Base Isolation

Base Isolation prevents the transfer of seismic forces from ground to the superstructure by decoupling the whole structure from the ground [11]. The decoupling is achieved by inserting a flexible layer, having low stiffness with respect to the superstructure at the base known as Base Isolator. This layer provides flexibility and energy dissipation mechanism to the structure [12]. Base isolation is intended to be perfectly elastic so that the building is restored to its original position after a seismic event [13]. The main concept of Base Isolation is to increase the time period of the structure which in turn reduces the accelerations and earthquake forces experienced by the structure [13-16]. By allowing the system to vibrate with earthquake accelerations, forces and Inter story displacement can be significantly reduced and the structure experiences a rigid body motion. However, this also increases the Base drift significantly. One way to get around is to introduce some stiffening element. This type of Hybrid system works effectively for some earthquakes while remaining susceptible to others [17].

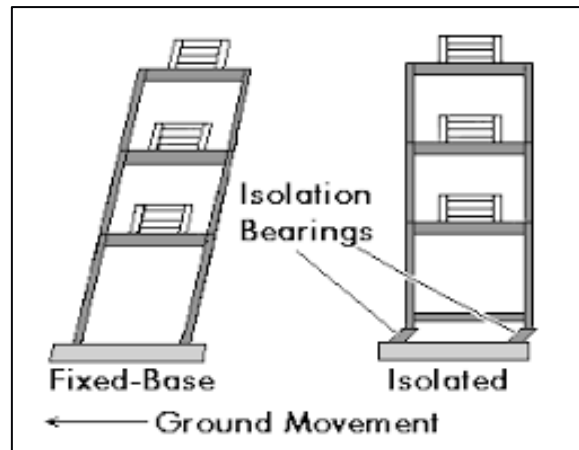


Figure 2: Behavior comparison of Fixed base and Isolated Base System

1.2 MRE in Base Isolator

Magneto-rheological Elastomer (MRE) is a multifunctional smart material that consists of an elastomer matrix studded with magnetically sensitive particles. Its distinguishing feature is its tunable shear modulus, which may be obtained by applying a magnetic field [18]. When this field is removed, the substance returns to its former state with ease, demonstrating its reversibility. Depending on the degree of the magnetic flux applied, MRE can easily transition from a supple elastomeric state to a semi-solid shape [19].

MREs have sparked tremendous interest across a wide range of engineering disciplines by capitalizing on these distinguishing characteristics. Their integration has cleared the way for breakthroughs in a wide range of applications, from vibration absorption and isolation devices to controlled valves and adaptive beam constructions [20, 21]. Furthermore, MREs have the potential to be used in smart braking systems and haptic devices, suggesting unique ways to improve both automotive safety and human-machine interaction [22].

Notably, MREs have attracted substantial interest in the sphere of civil engineering, notably in the context of base isolation systems. [17, 23] Researchers have been drawn to them because of their potential to solve the shortcomings of passive and hybrid isolation techniques [24, 25]. This idea revolves around MREs' ability to dynamically adapt their mechanical properties in response to applied flux, hence contributing to structural damage mitigation and reinforcing civil infrastructure's seismic resilience [26].

The attractiveness of Magneto-rheological Elastomers lies in its capacity to transcend standard material behavior constraints, ushering in a new era of engineering possibilities.

Base Isolators can be installed in new as well as in old structures. The old structures can be retrofitted in locations of high seismic activity. The court of Appeals in San Francisco was retrofitted after a major earthquake while important structures like Daxing International Airport China was constructed with Base Isolator as seismic mitigation technique.

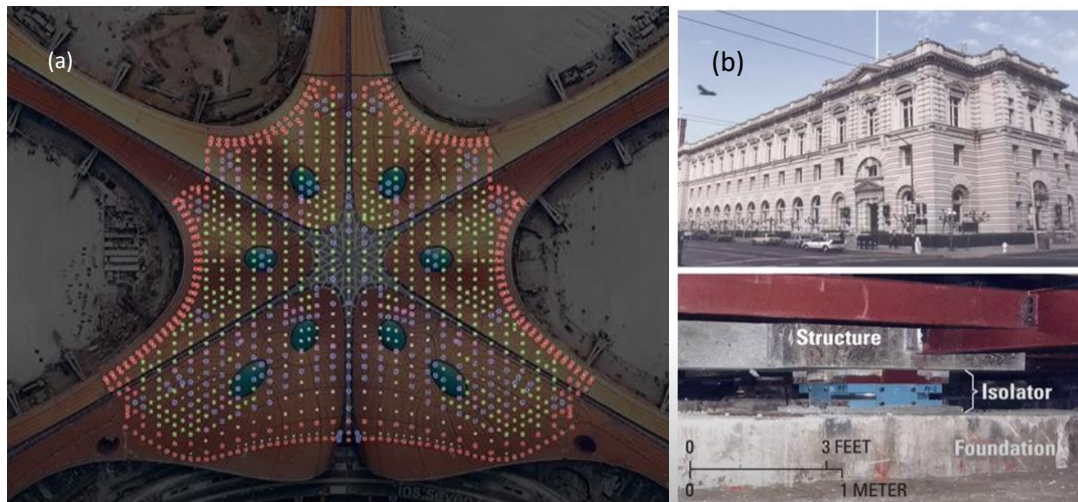


Figure 3: Examples of Base Isolated buildings (a) Daxing International Airport, China (b) Court of Appeals, California, USA

1.3 Fundamentals of Base Isolation

To have an effective system of Base Isolation, following criteria should be met:

1. It should reduce the horizontal acceleration of the structure due to earthquake.
2. It should not be responsible for any amplification in vertical acceleration.
3. Base drift should be low.

1.4 Problem Statement

Because of its large base drift, Base Isolators have a clear weakness. Increasing the stiffness will reduce this drift, but it may negate other critical benefits of the isolator such as story drift, maximum displacement, story acceleration, and so on, and push the entire assembly towards a fixed system. Various techniques have been used to reduce this base drift. A viscous damper was fitted in a friction pendulum system to successfully reduce base drift as well as story displacements [27]. Many control systems for MRE-based base isolators have been developed to provide the requisite stiffness to suppress these structural response characteristics while simultaneously managing base drift [28, 29]. These systems have been numerically validated. The MRE-based base isolator with a decreased scale structure needed to be evaluated under dynamic load to see how effective it was in reducing base drift and other response parameters.

The MRE is combined with nano and micro particles to create a hybrid elastomer; this hybrid elastomer is thought to be more efficient.

1.5 Research Objectives

1. To design and fabricate a reduced-scale MDOF frame.
2. To design and fabricate a variable stiffness Base Isolator.
3. To investigate the change in stiffness with different magnetic flux levels.
4. To Perform Dynamic testing on isolated system having variable stiffness

1.6 Scope of Research

This research is aimed at the development of a variable stiffness Base Isolator and the study its rheological properties with the change in magnetic Flux. This large-scale base isolated system is investigated under harmonic excitations.

1.7 Thesis Organization

The first chapter provides the introduction of earthquake phenomenon, its hazards, earthquake mitigation technique, Base isolation and MREs employed as smart material for seismic mitigation. The second chapter discusses the available literature on MRE based Base Isolator. The third chapter encompasses methodology employed in carrying out the research as well as the materials and equipment employed in this research. The fourth chapter deals with the results and discussion of the study. And Fifth chapter presents concluding remarks drawn from this study.

Chapter 2: Literature Review

Base isolation is an innovative approach that decouples a building from ground motion, reducing its vulnerability to seismic forces [30]. Base isolation provides superior protection compared to dampers by effectively isolating the building from seismic forces [29]. The base isolators are deliberately positioned at the foundation of a structure in order to enhance its flexibility and capacity for dissipating energy [12]. Through this action, they are able to reduce the negative impacts caused by seismic forces [31].

2.1 Types of Base Isolators

Numerous categories of base isolators have been devised with the objective of augmenting the seismic resistance of structures. These isolators provide unique techniques for collecting and dissipating seismic energy, so protecting buildings and infrastructure from the harmful consequences of ground motion. Lead rubber bearings, sliding bearings, and elastomeric bearings are notable types that exhibit distinct features and offer various advantages [32].

Lead rubber bearings are designed to utilise the intrinsic damping characteristics of lead and rubber materials. In this configuration, the lead core plays a pivotal role in providing necessary damping, effectively absorbing and dissipating seismic energy [9]. The system's capacity to dampen vibrations and facilitate controlled movement during seismic occurrences is enhanced by the rubber component's inherent flexibility [33]. The combination of lead and rubber exhibits a synergistic effect that proves to be a highly efficient method for mitigating the dynamic pressures exerted by earthquakes, hence improving the overall seismic performance of structures.

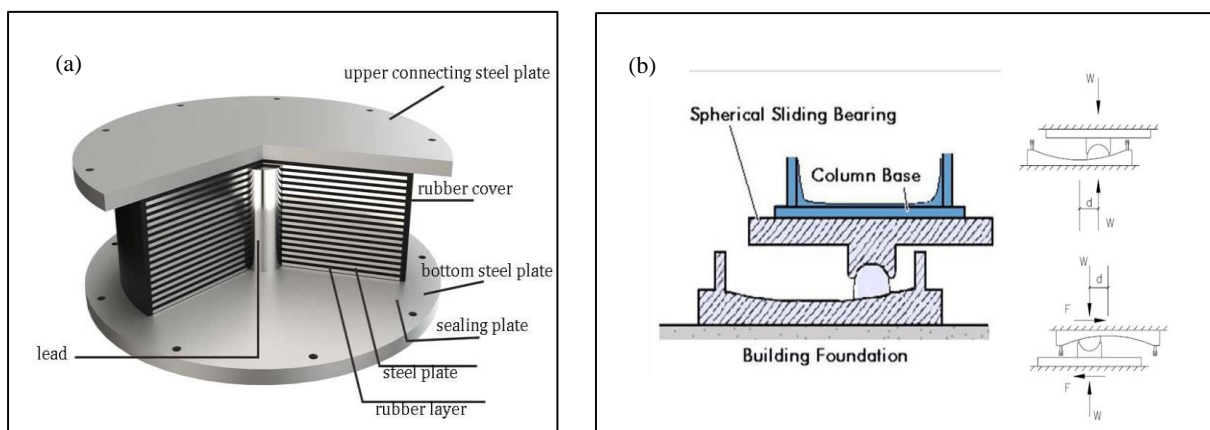


Figure 4:(a) Typical schematics of Lead Rubber Bearing (b) Typical schematics of Sliding Bearing

The inclusion of sliding bearings in a structural system results in a notable self-centring characteristic, which plays a vital role in preserving the structural stability when subjected to seismic forces. The design features the integration of a spherical ball that is situated within a concave surface. The presence of a curved concave contact allows for unrestricted movement of the ball in reaction to ground motion, hence aiding a self-centring event [34]. The intrinsic attribute of the bearing enables it to readjust its position following horizontal displacement, hence reducing the likelihood of damage caused by displacement. Sliding bearings possess the advantageous combination of lateral flexibility and self-centring characteristics, rendering them a resilient alternative for seismic mitigation.

In contrast, elastomeric bearings utilise the combined characteristics of steel and rubber within a composite configuration. The aforementioned bearing type is comprised of alternating layers of steel and rubber, meticulously fused together in a sandwich-like configuration. The steel layers serve the purpose of providing load-carrying capability and structural support, whereas the elastomeric layers contribute to the attributes of flexibility and energy absorption. Through the amalgamation of these materials, elastomeric bearings have the capacity to provide markedly enhanced load-bearing capacities in comparison to a solitary elastomer. This characteristic enables structures to endure greater vertical loads while also maintaining the requisite flexibility for accommodating seismic movement [35].

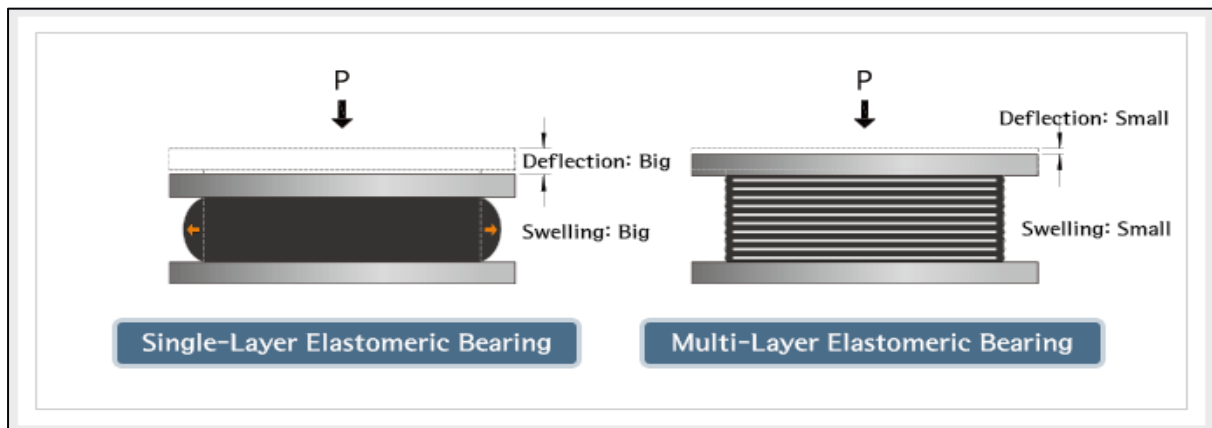


Figure 5: Comparison of Single-Layer and Multi-layer Elastomeric Bearing

Essentially, these various forms of base isolators are designed to address distinct seismic issues. Lead rubber bearings prioritise the efficient dissipation of energy, whereas sliding bearings demonstrate exceptional self-centring behaviour. Elastomeric bearings, on the other hand, leverage their load-carrying capacity and flexibility to their advantage. The choice of a certain type is contingent upon the structural demands, the expected seismic events' size, and the

desired performance goals. Engineers have the ability to customise seismic protection solutions for various structural designs and environmental situations through the utilisation of these inventive base isolators.

The damping qualities of rubber have an impact on the seismic reaction.

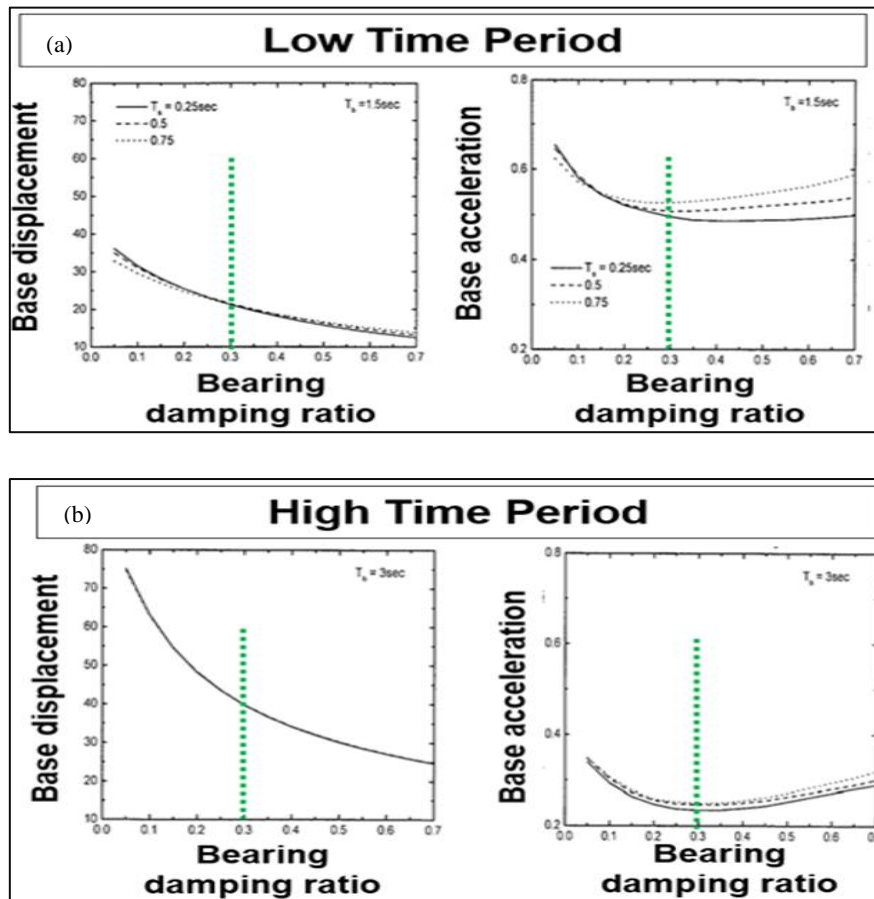


Figure 6: Base displacement and Base acceleration comparison of Base Isolator having (a) High Damping Rubber (b) Low damping rubber.

The presence of high damping results in a decrease in displacement and an increase in acceleration demands, whereas low damping leads to an increase in displacement and a decrease in acceleration requirements. This establishes a trade-off between these two factors. The dynamic relationship between damping and displacement holds significant significance for the field of earthquake design and the optimisation of structural performance.

2.2 Principle of Base Isolator

The technique of base isolation is employed to intentionally modify the inherent frequency of a system in order to mitigate resonance with seismic forces. Base Isolator increases the time period of the building thus decoupling the structure and returns to its original position after

seismic event [13-16]. Passive isolator, however once fitted cannot modify its stiffness [36]. The utilization of an isolator with adjustable stiffness is crucial for achieving effective isolation due to the varying frequency content of earthquakes [13, 37]. The active isolator enables the manipulation of the system's reaction in order to mitigate the impact of detrimental frequencies, resulting in a decrease in structural demands and an improvement in seismic resilience [18]. Variable stiffness isolators offer a flexible approach to mitigating the effects of various earthquake types by adjusting the stiffness in accordance with individual seismic demands [28].

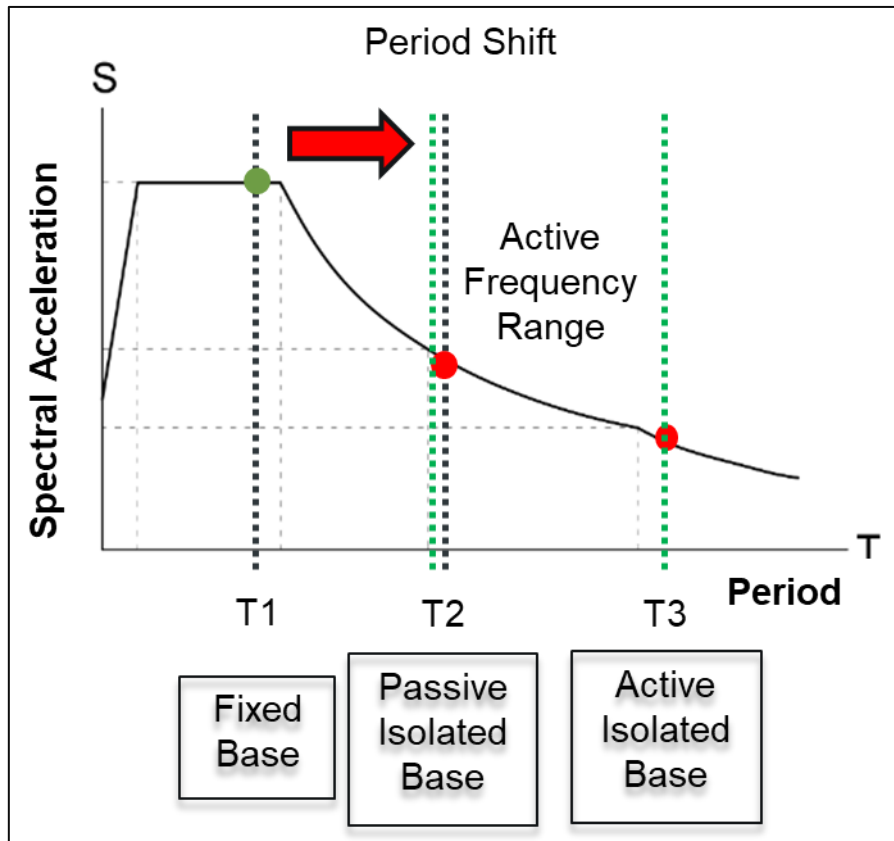


Figure 7: Effect of Variable frequency range of Active isolated structure on spectral acceleration

2.3 Smart Materials

The materials classified as magnetorheological (MR) belong under the realm of Smart materials, as their rheological characteristics can be manipulated by altering the external magnetic field that is applied [18]. MR materials consist of microscale iron particles that are scattered within an elastic matrix, which exhibits non-magnetic properties. The application of a magnetic field has the ability to induce quick and reversible changes in the rheological characteristics of these materials [28, 38-40]. The observed phenomena can be attributed to the alignment of magnetic particles that are present within the elastic matrix. MR material may

include fluids or elastomers. MREs offer many advantages over MRFs and are now used widely in different applications [28, 38, 41]. The advantages include:

- **Semi Solid State:** MREs often refer to elastomers or materials with rubber-like properties that exhibit a solid-state structure. The implementation of solid structures has several advantages, including enhanced integration with devices, decreased likelihood of leakage, and improved suitability for applications that prioritize containment or sealing. This contrasts with the liquid-based nature of MRFs, which sometimes necessitates the use of more intricate sealing mechanisms.
- **Adaptable Shape:** MREs can be manufactured in a variety of configurations, including those with complex geometries. This allows for greater flexibility in designing and incorporating MREs into a variety of devices, such as adaptive structures or wearable devices, which may not be possible with MRFs.
- **Large Variable Stiffness:** When compared to MRFs, MREs can have a bigger range of stiffness levels. This can be helpful in situations where a wider range of stiffness modulation is needed, like in vibration isolation systems or shock dampers.
- **Shape Integrity:** MREs tend to keep their mechanical integrity and structural stability even when they are subjected to high loads or shear forces. This can be very important in situations where heavy loads or dynamic forces are present. Since MRFs are made of liquids, they could have flow problems in similar situations.
- **Quick Response Time:** MREs can provide quicker response times than MRFs in some cases. This has potential benefits for real-time adaptive damping systems and other applications that benefit from quick changes in material properties.
- **Particle Deposition:** Magnetic resonance filters (MRFs) may experience a phenomenon known as magnetic particle settling, which can result in diminished efficacy and performance over a period of time. MREs, by virtue of their solid-state composition, exhibit a reduced susceptibility to problems associated with sedimentation.

2.4 Base Isolator limitations, and technological advancements in seismic mitigation

Base isolators are considered appropriate in situations where the subsoil does not generate prolonged periods of ground motion [14]. Research conducted using full-scale shake table experiments has demonstrated that base isolation systems are susceptible to seismic damage when exposed to long period ground motion and short period earthquakes with substantial

amplitudes [24, 25]. According to the literature, conventional base isolators are classified as passive systems that lack the ability to be altered or adjusted after installation [36]. This limitation restricts their capacity to adapt to dynamic local circumstances and the diverse spectrum of earthquakes they might encounter. Passive base isolation demonstrates effectiveness in controlled stress conditions, although its efficacy may be compromised in other contexts [13, 37]. The deformation of base isolators is limited due to the material properties [23]. The effectiveness of a passive base isolator's design is contingent upon the size and frequency of earthquakes. Consequently, traditional base isolators exhibit sensitivity to many types of earthquakes, including those occurring at a significant distance from the fault and those occurring in close proximity to the fault with large displacement [4-6]. Significant displacements resulting from far field earthquakes have the potential to cause the isolator to exceed its operational limits and cause the isolator to overstretch while short period earthquake with large amplitude may result in pounding effect thus transferring large impact forces to the structure [6].

Yundong et al [10], conducted a thorough examination focused on evaluating the extent of damage sustained by non-structural components within a hospital facility. The study conducted an empirical investigation to clarify the complex dynamics that impact the susceptibility of hospital infrastructure. During the occurrence of a long period seismic event the investigation revealed occurrences in which appliances within the structure experienced significant displacements, above a notable threshold of 3 meters. Moreover, the displaced appliances were subjected to substantial collision forces, quantified at 36 kN. In a similar manner, Bilal et al [14], conducted a thorough investigation on the consequences of seismic activity originating from both near and far fault earthquake sources on 3 different kinds of isolator. Interestingly, the results revealed that under the influence of far-field seismic excitation, the maximum displacement measured in a low damping rubber bearing system was higher than that of the non-isolated system. Bhandari et al [42], expanded their investigation to encompass the intricacies provided by short period ground motions characterized by directivity and fling-step effects. Particularly it was discovered that the structural stability of the base-isolated building frame may be compromised in the presence of near-field earthquakes accompanied by fling-step effects and the isolated system went into the inelastic range, even when subjected to lower levels of Peak Ground Acceleration (PGA). For the near-field earthquake with fling-step effect, the percentage reductions in the response quantities are considerably reduced, indicating that the base isolation proves to be ineffective for this type of near-field earthquake. Yunbyeonget

et al [43], conducted a study that aimed to improve Base-Isolation Systems by implementing Controlled-Damping Isolation (CDI) Systems. The implementation of CDI systems has demonstrated the possibility of attaining similar levels of isolator bearing deformation as high damping passive systems. Furthermore, the research findings suggest that the use of CDI systems resulted in a decrease in the requirements for story drift, velocity, and acceleration on the superstructure, in comparison to passive systems. This study presents a potential approach for enhancing seismic resistance by implementing novel control mechanisms without increasing the base drift of the isolator. Jianchun et al [39], introduced new formulations for an adaptive laminated Magnetorheological Elastomer (MRE) based Base Isolator. The research yielded two seismic isolator prototypes, each characterized by unique initial loading capacity and adjustable lateral stiffness values. One with high vertical load carrying capacity but with small adjustable lateral stiffness of 37.49 percent and other with small vertical load carrying capacity but with large lateral variable stiffness of 1630 percent. Furthermore, Xu Chen et al [27], used friction pendulum bearing (FPB) technology with viscous dampers (VD). The integration of VD in the proposed FPB-VD device resulted in a significant consequence, as it successfully reduced deformation demands in the isolation layer while also reducing the structural acceleration demands.

2.5 Advancement in MRE

MRE materials are those smart materials whose properties can be altered in the presence of a magnetic field [6, 28]. Magnetic particles, mostly carbonyl iron particles due to their advantages like greater saturation, less remanent magnetization is spread out in a flexible matrix [44]. They are dispersed in a flexible matrix and upon the application of magnetic flux can align themselves in the direction of the applied flux, making a chain like structure and increasing the stiffness of the MRE [45]. This chain like structure remains in its position as long as required flux is present [18].

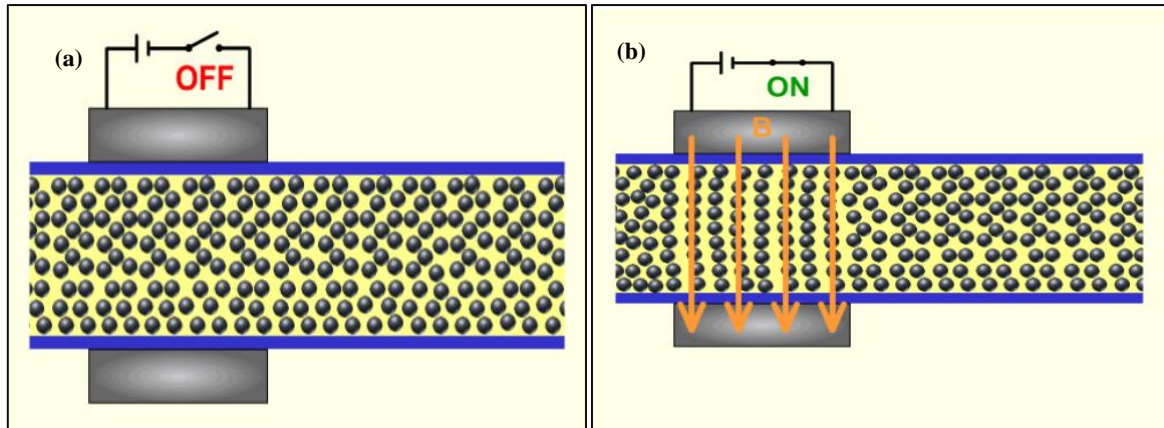


Figure 8: Magnetizable particles in MR system (a) without magnetic flux (b) with magnetic flux

After the removal of magnetic flux, the particles come back to their original position thus providing a material with variable stiffness as shown in figure 8. The historical progress in the field of Magneto Rheological (MR) can be attributed to Rainbow in 1940 [46]. This phenomenon served as the basis for further inquiries into the possibilities of MREs. Significant progress was achieved when Jolly et al, conducted a comprehensive investigation into Magneto Rheological Elastomers (MREs), illuminating their multifaceted characteristics. Significantly, the investigation demonstrated that the inclusion of 30% iron particles in the composite resulted in a substantial modification in modulus, ranging from 30% to 40% [46]. The measurement of the magnetorheological (MR) effect is commonly assessed by quantifying the change in modulus (G) under a specific magnetic field, compared to the initial storage modulus without any magnetic impact [38]. The relationship between shear modulus and magnetic field strength demonstrated a linear trend at first, ultimately reaching a state of saturation at higher field intensities [38].

Further experiments were carried out in calculating the change in shear modulus with the variation in applied magnetic flux. Zho et al, experiments revealed the possibility of dynamic modulus variations that may reach 50%, while Gong et al, suggested an even more significant potential exceeding 100% [47]. It is worth mentioning that MREs represent a different class of intelligent materials, which should be distinguished from Magnetorheological Fluids (MRFs). MREs have similarities to MR fluids in terms of their mechanical behavior, yet they possess unique characteristics. Magnetorheological fluids (MRFs) exhibit a dependence on the applied field for their yield stress, whereas magnetorheological elastomers (MREs) demonstrate a dependence on the applied field for their shear modulus [38]. The materials used in MREs have

similarities to viscoelastic substances in the pre-yield region [48]. However, there are differing viewpoints on the impact of magnetic fields on the damping qualities [49].

The variable stiffness of MREs makes them well-suited for use as base isolators in structures and bridges [50]. The composites are carefully fabricated, consisting of ferromagnetic fillers embedded inside an elastomeric matrix, accompanied by additives [38, 44]. After curing, the filler particles tend to align themselves in accordance with the direction of magnetic flux. This alignment contributes to the magneto-rheological (MR) effect, which enhances the mechanical properties of the material [45]. Significantly, there has been a considerable amount of research conducted on the customization of factors such as particle properties, matrix material, and additives [51]. The properties of the elastomer are significantly influenced by the matrix material, which is a non-magnetizable viscous gel [52]. Rubber was used in earlier era as the composite material however silicone rubber in comparison to natural rubber is preferred now. This preference can be linked to silicone rubber's ability to allow easy particle movement, improved performance under high temperatures, and superior tensile, compressive, and tear strength [53, 54].

Magnetizable particles are embedded in the matrix. These particles also increase the initial stiffness of the elastomer at zero magnetic flux. Iron particles are usually selected due to their notable magnetic characteristics [44]. The presence of substantial content enhances the MR effect as a result of its closer proximity [55]. Research indicates that it is beneficial to match the particle content with the critical particle volume concentration (PVC) in order to achieve optimal performance [50].

Nanoparticles have been identified as significant factors that enhance the effectiveness of MREs under conditions of increased stress and decreased flow values [50]. The utilization of nano-particles promotes the achievement of uniform magnetization, consequently leading to the enhancement of multiple characteristics [56]. The modular characteristics of magnetized particles enable the enhancement of the MR effect through facilitating linking [44]. The study conducted by Palacio focuses on the integration of nano and micro-sized particles in elastomers, highlighting the enhancement of mechanical and magnetic properties in magnetorheological elastomers (MREs) through the use of nano-fillers. Additionally, the study reveals that increased cross-link density leads to improved elongation in MREs [50]. Interestingly, the utilization of nonmagnetic particles in conjunction with magnetized counterparts presents an intriguing opportunity for enhancing particle chains, hence providing

a unique pathway for optimization [57]. The observed increase in stiffness might be ascribed to irregular structure and optimal arrangement, hence enhancing moduli and viscosity [58].

Chapter 3: Methodology and Material

This chapter presents the methodology, material and experimental setup employed in the fabrication and testing of an isolated system. Various materials, procedures, and tools used to create, put together, and experimentally evaluate the base isolator are discussed in this chapter. Steel plates, steel laminations, elastomer, and magnetic coils are the four main parts of the base isolator. A reduce scale 3-Dof structure is used which after the insertion of isolated layer can be treated as 4 DOF structure. M_1 , M_2 and M_3 are the lumped mass of the storeys while K_1 , K_2 and K_3 are stiffness of storeys. K_b and M_b represent the stiffness and mass of base isolator respectively as shown in figure 9.

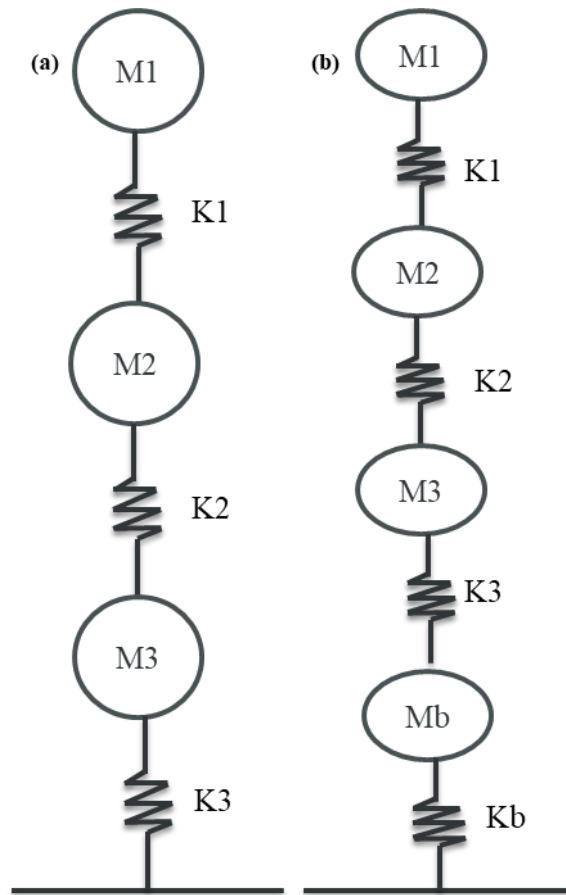


Figure 9: Simplified MDOF representation of the models studied (a) Fixed Base system (b) Isolated Base system.

Three important parameters are identified for an active Base isolator. Its vertical load carrying capacity, initial lateral stiffness, and its variable stiffness range. The load carrying capacity is calculated by the formula present in literature [39]. This formula is dependent on its shape and diameter as well as its material properties. The weight of the structures supported by the isolator is first calculated and depending upon this weight the base isolator shape and dimensions are

finalized. After finalizing the dimensions of steel laminations, other steel components of Base isolators are finalized with FEMM analysis. FEMM analysis presents the amount of current required to produce magnetic flux depending upon different configuration of steel components as well as the diameter of wires and no. of turns around an electromagnetic coil. This coil is capable of producing magnetic flux.

Elastomers are then fabricated and placed in a laminated manner with steel plates of the same size and shape to support vertical loads and to provide support to elastomers against bulging. Elastomers consist of a matrix, some magnetizable particles and additives. The additives used help in homogeneous mixing of the iron particles in the matrix by reducing the friction and providing ease of movement. A lot of research has been carried out to optimize the size and concentration of these components in elastomer to prepare maximum magnetic flux. Nano particles are also incorporated with micro iron particles to enhance magnetic flux. The composition of elastomer was picked from a previous study [50] producing maximum variable stiffness. All components are then assembled to fabricate Base Isolator.

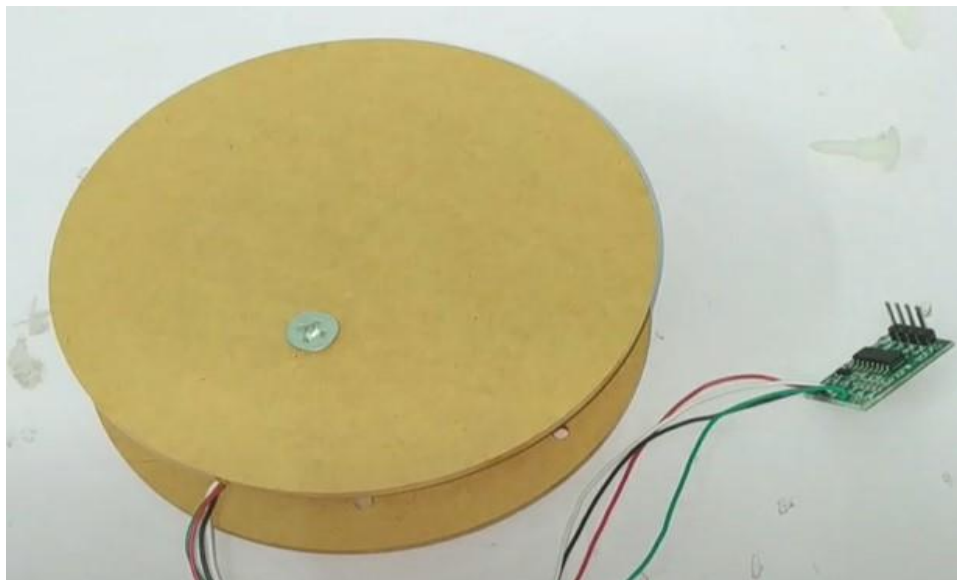


Figure 10: Arrangement fabricated for the calibration of Load Cell

Stiffness of Base Isolator is calculated using shake table. LVDT is calibrated against measured displacement first. The load cell is also calibrated against some predefined load as shown in figure 10. After calibration, the load cell is fixed to the top plate which is fixed to some solid reference and LVDT is fixed with shake table. The combination of load measured, and displacement obtained provide stiffness. This test is repeated several times against different currents to calculate variable stiffness of active Base isolator. MATLAB calculation provides

the mode shapes, time period and frequency of active isolator by inserting different values of stiffness in isolation layer measured from previous tests.

Dynamic testing is then performed to analyze the seismic response of the isolated structure against different sinusoidal excitations. The stiffness of Base isolation was varied by varying the current from DC supply. Optimum stiffness was calculated against various frequency and amplitude for Base story reduction, Story drift reduction, maximum displacement and acceleration reduction. Following sinusoidal excitations were applied to the shake table.

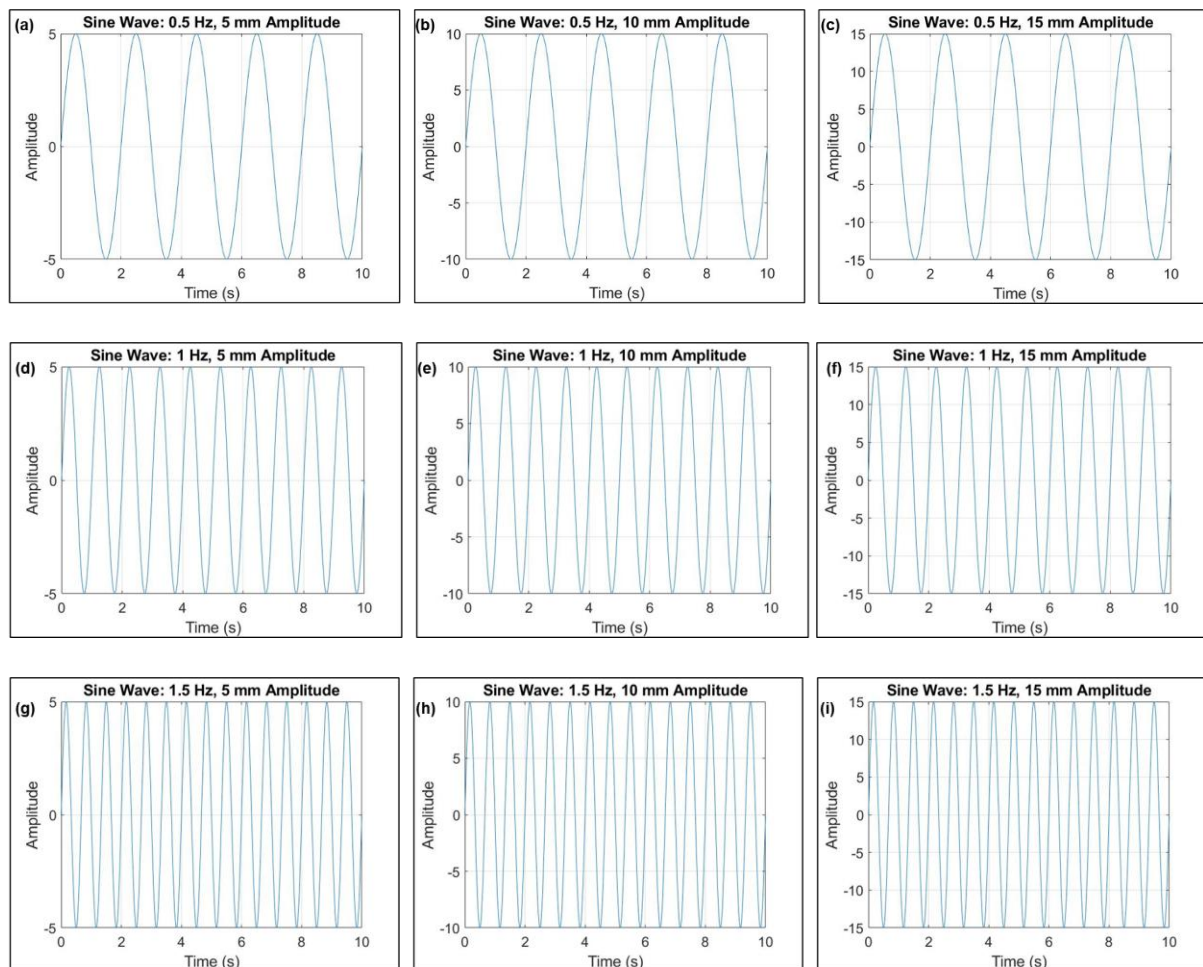


Figure 11: Loading Time Histories applied for different cases (a) 0.5 Hz, 5mm (b) 0.5 Hz, 10mm (c) 0.5 Hz, 15mm (d) 1Hz, 5mm (e) 1Hz 10mm (f) 1Hz, 15mm (g) 1.5 Hz, 5mm (h) 1.5Hz, 10mm (i) 1.5Hz, 15mm

3.1 Elastomer Size

The size of the base isolator depends on the vertical load carrying capacity. As the base isolator has large vertical loads, it is important that the base isolator can support these loads. A laminated structure works best in this scenario restricting the rubber or elastomer from bulging out. The formula for the size of base isolator is given below.

$$W = A.G.S.\gamma w$$

Where ‘W’ is the vertical load carrying capacity, ‘A’ is the overlapping area after given the maximum strain. ‘G’ is the shear modulus; ‘S’ is the Shape factor and ‘ γ_w ’ is the density of iron particles used.

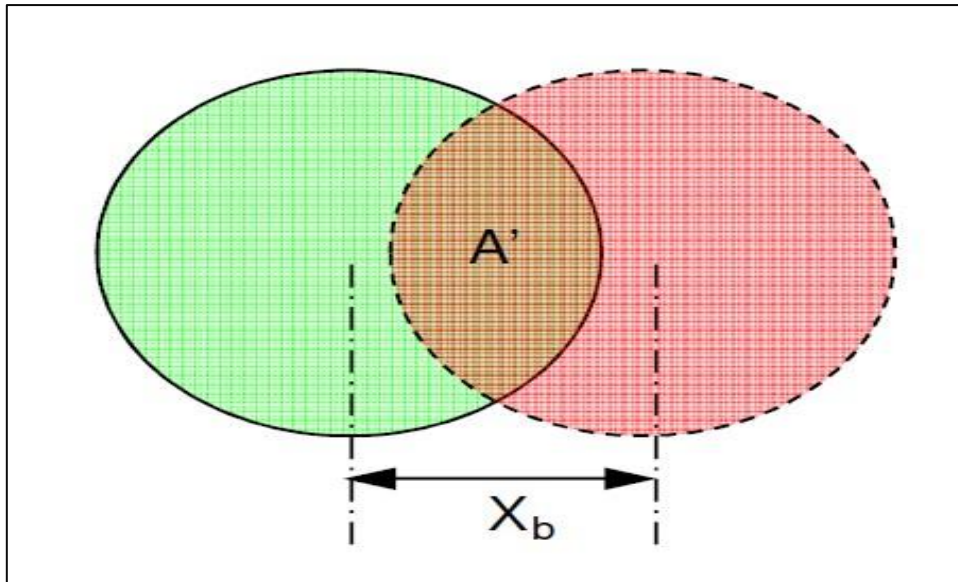


Figure 12: Overlapping Area (A) of the top and bottom plates of the isolation bearing in fully deformed state.

‘A’ is the overlapping area between the top plate and bottom plate after given a maximum strain. Strain is a limiting factor here as more strain causes the particles to drift apart resulting in decrease of shear modulus. [55, 59]. The limiting strain can be found out as the function of height. Jian chun li et al, used a strain having a ratio of 0.27 with the vertical for normal isolator, while for soft isolator a strain with the ratio of 0.6 was used [39]. This area can be calculated on AutoCAD. The shear modulus of rubber or elastomer as well as the density of filler particles used in the study are usually provided by the vendor. The shear modulus can also be calculated by preparing a sample modal of the elastomer or rubber and then using a rheometer. ‘S’ is the shape factor that depends on the shape of the elastomer. For a round shape the shape factor can be normalized to $\phi/4(t)$ where ϕ is the diameter of elastomer.

3.2 Optimized Sized of Elastomers

A 2-D FEMM analysis was performed in order to optimize the size of various steel components and to guarantee maximal flux around the laminated layers. FEMM is ideally adapted for analysis of magnetic fields. It can precisely calculate magnetic flux density, magnetic field intensity, and magnetic losses. FEMM contains numerous post-processing tools for analyzing and displaying simulation data. The surrounding environment and elastomers were regarded as

air, and the area was sealed off. Several experiments utilizing various sizes of top and bottom plates, steel yokes, wire diameter, and number of turns in the electromagnetic coil were conducted, and the dimensions with the highest performance within the working range were selected. The visualization tools assisted in the development of an optimal design.

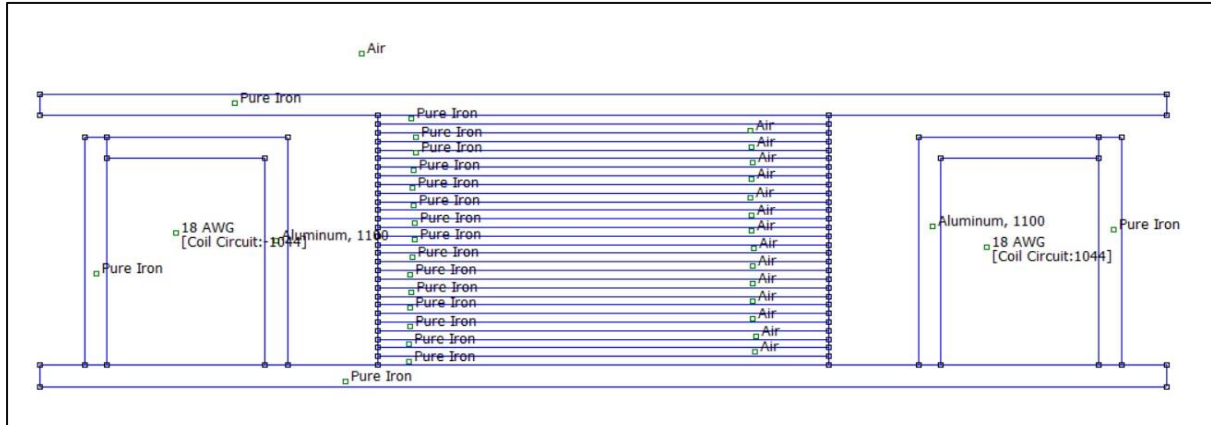


Figure 13: Finite Element Method Magnetics (FEMM) model for optimizing sizes of various steel components for maximum magnetic flux.

During these tests, a noteworthy observation was made as well. Although increasing the size of the wire increases ampacity, and increasing ampacity increases magnetic flux, increasing the size of the wire reduces the number of turns. In other terms, if we had 5 amps of capacity, the number of rotations would have been reduced. Using a short wire with an ampacity of 4 amps and a large number of turns (over 1000 turns) produced greater magnetic flux.

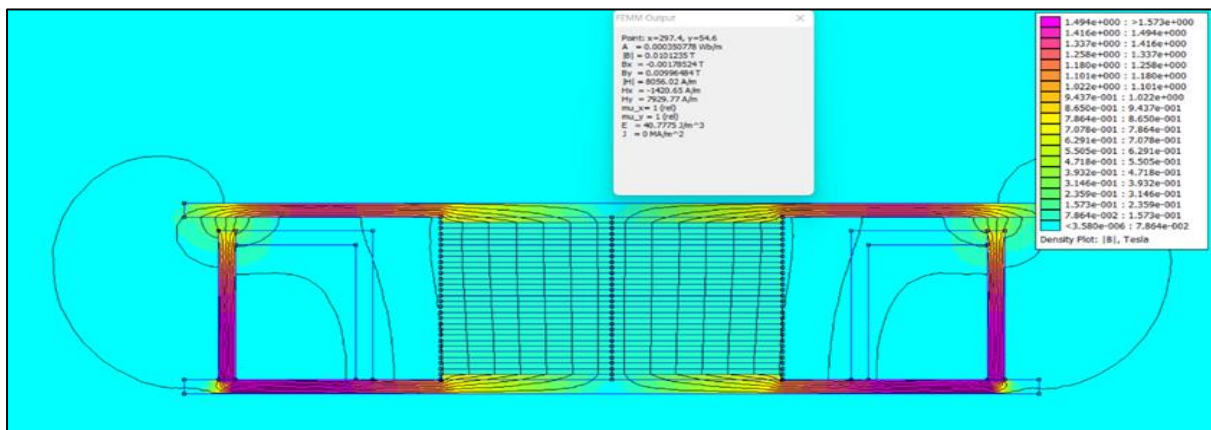


Figure 14: Magnetic flux contours obtained from FEMM for optimized size of steel components.

Uniform magnetic flux was achieved throughout the base isolator assembly. FEMM results were used to optimize the size of different steel components as well as the size and no. of turns of wire used. A uniform magnetic flux of 0.12 Tesla was achieved at 4 Amp current. This magnetic flux was different for different currents.

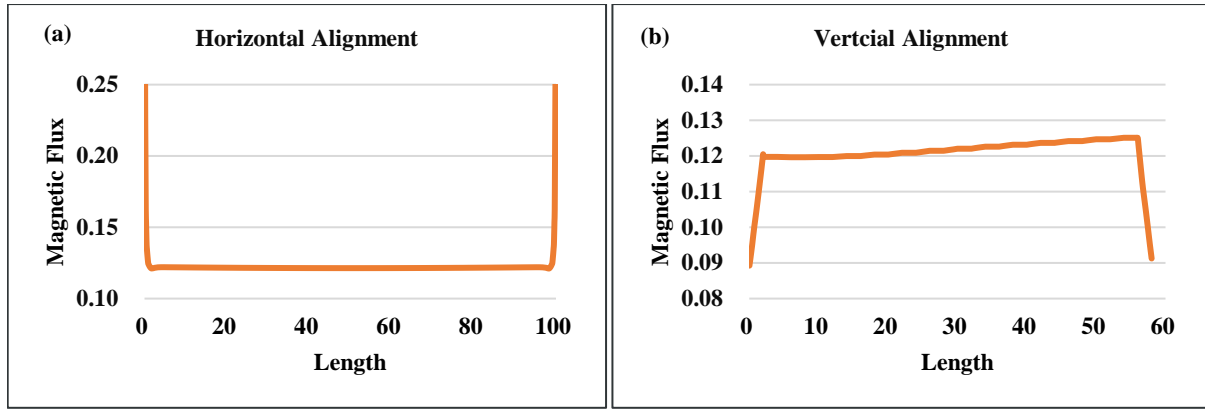


Figure 15: Variation of magnetic flux along (a) Horizontal Axis (b) Vertical Axis

Table 1: Optimized Components of Base Isolator assembly

Steel Component	Diameter (mm)	Thickness (mm)
Top Plate	250	5
Bottom Plate	250	5
Steel Yoke	230	5
Laminated Steel Plates	100	2

Details of different components of Base Isolator are provided below:

3.3 Electromagnetic Coil

The laminated assembly is encircled by an electromagnetic coil. The coil is composed of a non-magnetic reel with a diameter ranging from 150mm to 220mm and a thickness of 5mm. This reel is made using POM plastic material, and the magnetic wire is coiled around it. The magnetic wire has a diameter of 1.15mm and has an ampacity ranging from 2.4 to 4 Amp. The non-magnetic reel can house more than 1000 turns. The application of an electric current to this electromagnetic coil results in the formation of the magnetic core. This core, along with the laminated structure, the top plate, the bottom plate, and the steel yoke, collectively establish a closed pathway for the magnetic flux.

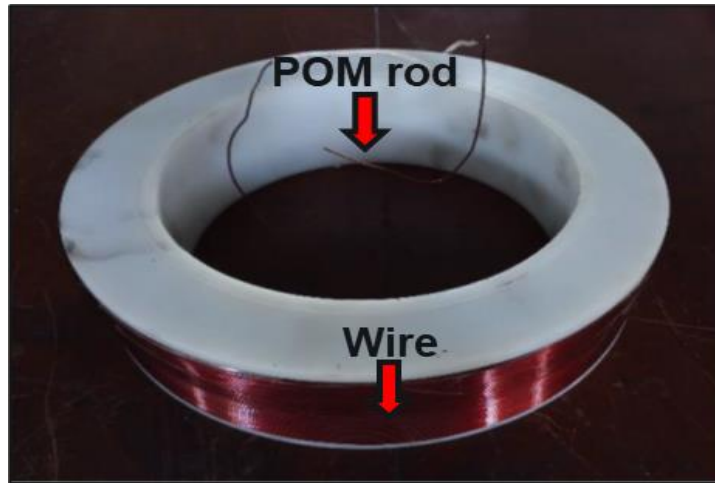


Figure 16: Electromagnetic Coil for providing magnetic flux to whole assembly.

The variation of magnetic flux with current can be seen in the graph. As current increase magnetic flux increases. The magnetic flux can be increased by increasing the size of wire thus increasing its ampacity or by increasing the number of turns. The no. of turns can be increased by decreasing the size of wire. Hence optimization is achieved considering both these effects.

Table 2: Optimized Electromagnetic Coil dimensions

Inner Diameter	150mm
Outer Diameter	220mm
Wire Gauge	17AWG
Ampacity	2.4-4Amp
Number of Turns	1067
Non-Magnetic Coil Material	POM rod

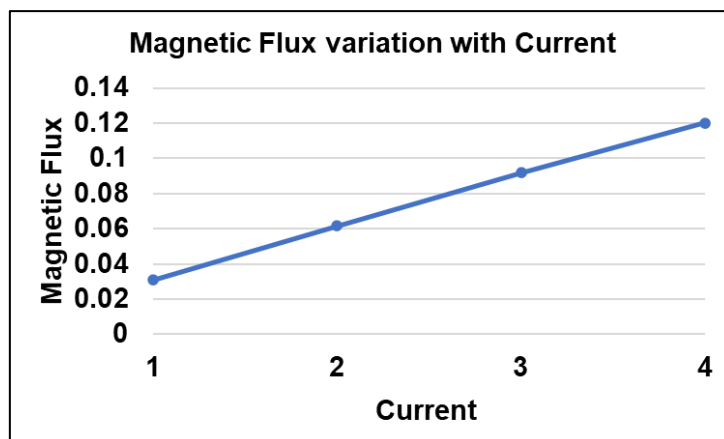


Figure 17: Magnetic Flux variation with Current

3.4 Steel Components

Top Plate and Bottom Plates are used to connect the isolator with the frame and the shake table respectively.

3.4.1 Top Plate

The primary function of the Top Plate is to bear vertical loads from the upper portion by serving as a stable platform for the top structure, typically composed of a Steel Frame. The steel frame is securely fastened to the top plate using bolts. The bonding of laminated steel plates and elastomers to the top plate is achieved through the use of an epoxy adhesive. The dimensions of the top plate, specifically its diameter and thickness, are contingent upon the optimizations performed on a Finite Element Method Model (FEMM) of the base isolator.

The aforementioned factors are dependent upon the diameter of both the laminated structure and the steel yoke, given that the top plate encompasses the entire assembly. A steel plate, with a diameter of 250mm and a thickness of 5mm, has been selected based on considerations of the steel yoke and electromagnetic coil dimensions, as well as through rigorous Finite Element Method Magnetics (FEMM) study.

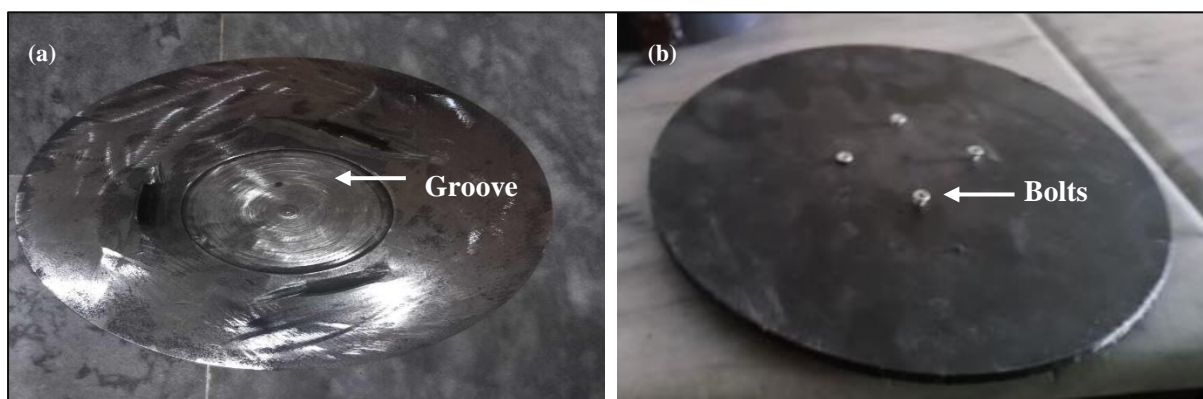


Figure 18: (a) Top Plate used in fixing Base Isolator to Steel Frame (b) Bottom Plate used in fixing Base Isolator to Shake Table

3.4.2 Bottom Plate

The use of Bottom Plates facilitates the secure attachment of the entire system to the Shake Table. The transfer of horizontal forces from the Shake Table to the Base Isolator occurs via the connection established by the Bottom Plate. The entire assembly is enclosed by the Bottom Plate, and its dimensions are determined by both the Finite Element Method Magnetics (FEMM) and geometric limitations. Clampers are utilized within the bottom plate to secure the

Steel Yoke in its designated place. A steel plate measuring 250 mm in diameter and 5 mm in thickness has been given. The bottom plate provides structural support for the whole assembly of the base isolator.

3.4.3 *Steel Yoke*

The incorporation of a steel yoke within a base isolator provides numerous advantages. It serves to optimize the creation of magnetic fields, hence boosting the responsiveness of the magneto-rheological (MR) effect and permitting effective control over the stiffness of the material. Additionally, the use of a steel yoke within the isolator assembly serves to enhance its structural integrity, supporting various components and thereby guaranteeing resilient performance when subjected to seismic stresses.

Finally, the steel yoke assists in the establishment of a homogeneous magnetic field, facilitating constant and predictable modifications in the mechanical characteristics of the material.

A steel yoke, measuring 230 mm in diameter and 5mm in thickness, is included for the purpose of enclosing the laminated construction and electromagnetic coil. The Yoke remains in its position with the use of studs located in the Base Plate. The determination of an optimized size is concluded subsequent to the Finite Element Method Magnetics (FEMM) examination.



Figure 19: Steel Yoke employed for enclosing whole assembly.

3.4.4 Steel Lamination

The isolator utilizes the laminated structure commonly found in conventional rubber bearing isolators. Fourteen MRE sheets, each measuring 2 mm in thickness, are fixed to sixteen steel plates that are 2mm thick.



Figure 20: Laminated Base Isolator with alternating elastomeric and steel layers

The laminated structure offers several benefits, including the ability to bear heavy loads in the vertical direction, preventing lateral bulging of the rubber, and attracting magnetic flux towards itself and the non-magnetic elastomer sheets. These characteristics contribute to the laminated structure's high magnetic conductivity.

3.5 Elastomers

Elastomers were fabricated using Silicon rubber (Part A and Part B) together with silicon oil and Magnetizable particles (Nano and Micro Iron Particles). The mix proportion of Elastomer for optimize magnetic flux was picked from a previous study down by [50]

Table 3: Optimize Mix proportion of elastomer for maximum magnetic flux.

Silicon Rubber	8.125ml
Silicon Oil	2.708ml
Micro Iron Particles	11.5g
Nano Iron Particles	11.5g
Iron Particles by Volume	40 percent

3.6 Silicon Rubber

Silicon rubber has been utilized in the production of elastomer as an elastic matrix. Using silicon rubber was primarily motivated by the fact that the MR phenomenon can be observed significantly in silicon rubber-based elastomer. Silicon rubber consists of two parts, Part A and Part B. Part A acts as an elastomer that can be molded in different shapes and Part B acts as hardener. Both parts are mixed in the same proportion and after 24 hours a semi solid elastomer is achieved. Silicon Rubber was acquired from China's ShenZhen Hong Ye Jie Technology Co. It is primarily used for creating molds. Table lists the technical parameters of silicon rubber.

Table 4: Properties of Silicon Rubber used in elastomer.

Model	HY-E605
Colour	Translucent
Hardness	5 ± 2 Shore A
Curing Time	4-5 hrs.
Tensile Strength	3.5 ± 1 MPa
Viscosity	12 ± 5 kN/m
Shrinkage Rate	3000 ± 1000 mPa.s
Elongation	400%



Figure 21: Silicon Rubber (Part A and Part B) and Silicon Oil

20 percent Silicon oil is added together with Silicon rubber and iron particles to ease the production of a homogenous mixture. Silicon oil acts as an additive, reducing the friction between iron particles. After magnetic flux is applied, silicon oil lubrication also helps the iron particles in aligning along the direction of applied flux thus increasing MR effect. Silicon oil also facilitates increasing the response time of base isolator.

3.7 Iron Particles

The iron particles were obtained from MEIQI INDUSTRY & TRADE CO., LIMITED. The existing body of literature indicates that Hybrid Carbonyl Iron particles exhibit an increased Magnetic Resonance (MR) phenomena when subjected to the same applied flux. Iron particles having a size range of 3-5 μ m and 200 μ m were utilized in the fabrication of a hybrid elastomer, wherein the volume concentration of iron particles was set at 40 percent.

Table 5: Chemical Composition and Physical Properties Comparison

Item	Standard	Test Results
Fe	≥ 99.5	99.51
C	≤ 0.03	0.027
O	≤ 0.04	0.32
Tap Density,	4.0-4.4	4.26
Apparent Density	2.0-3.0	2.05

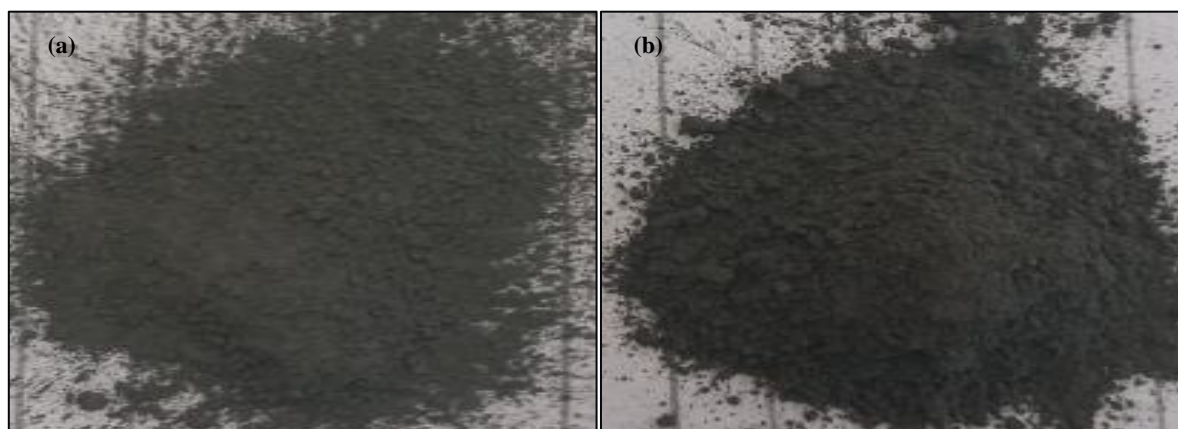


Figure 22: (a) Micro Sized Iron Particles (b) Nano Sized Iron Particles

An elastomer consists of matrix and magnetizable particles. Silicon rubber acts as the matrix, iron particles act as magnetizable component while silicon oil facilitates the mixing of iron particles in the matrix. Silicon rubber part A, Silicon oil and iron particles both nano and micro are first mixed in a flask. The mixture is then placed in a sonicator for thirty minutes creating a homogenous mixture.

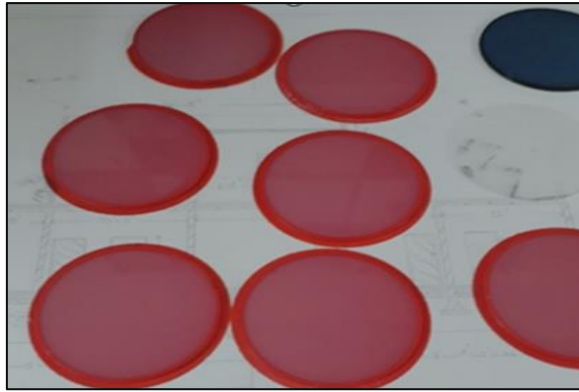


Figure 23: 3-D printed mould for casting elastomer layers.

To confirm the size of the elastomer a specially made 3-D printed mold is prepared. This mold should be made from the material that does not react with the matrix. Curing is said to be done if the elastomer does not leave any mark on the finger. This usually occurs after 24 hours. The elastomer can then easily peel off from the mold confirming to the required diameter and thickness.

Twenty-eight elastomers were cast, 14 for each elastomer. The elastomers are bonded together with the iron plates using epoxy. This sandwiched arrangement allows for large vertical load carrying capacity and greater protection against bulging out of rubber particles.

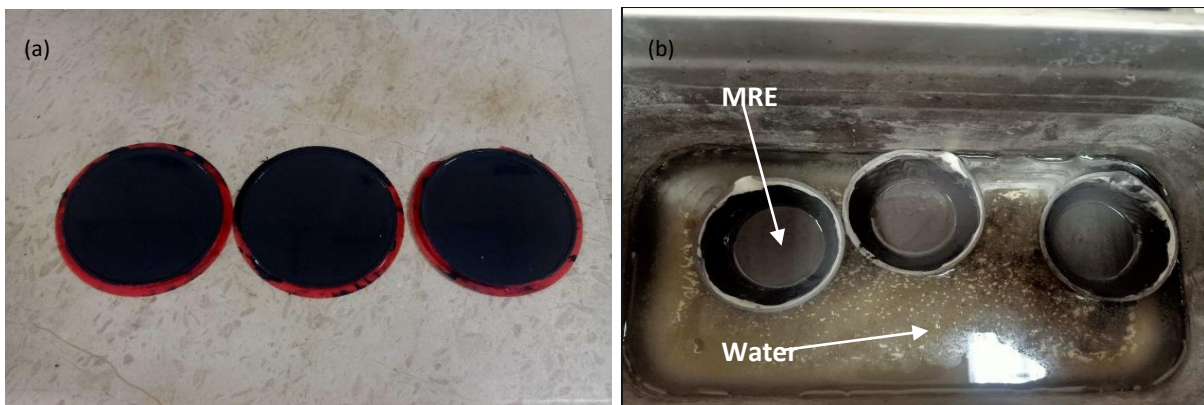


Figure 24: (a) Casting and curing of MRE layers (b) Sonification for homogeneous mixture of MRE.

3.8 DC Supply

DC Supply is used to provide direct current to the whole assembly. The DC supply is capable of providing variable voltage. The quantity of voltage required depends upon the resistance from the coil. A relationship between applied voltage and resultant current was obtained.

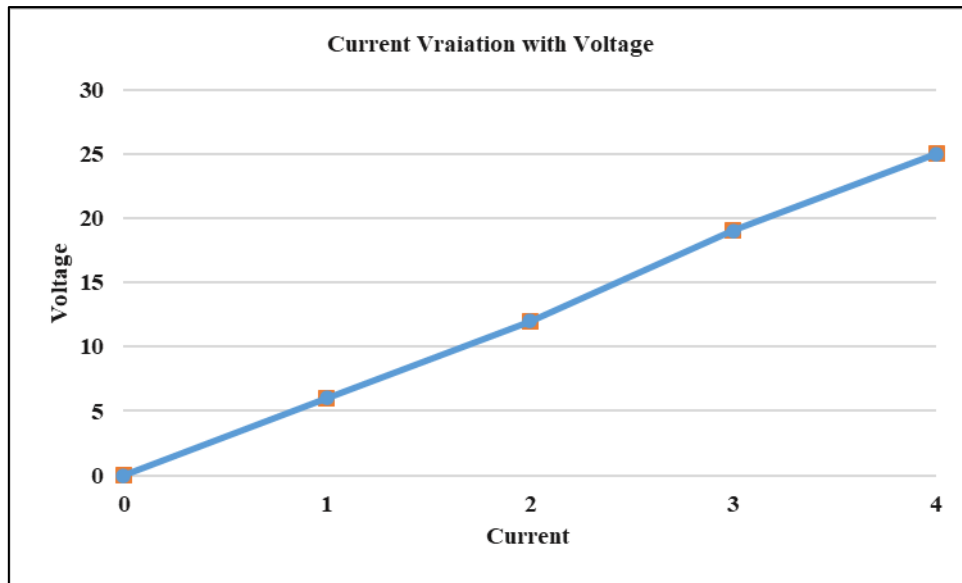


Figure 25: Direct Current (DC) Variation with Voltage having electromagnetic coil as resistance.

Before Dynamic testing, the stiffness of the base isolator as well as the natural time period and frequency of the isolated system is calculated to help understand the response of dynamic tests.

3.9 Stiffness Calculation

The MRE base isolator is firmly mounted above a shaking table for experimental testing, and its base movement is synchronized with the vibrations of the shake table. The load cell and the top plate of the isolator stay motionless during testing, thereby minimizing any undesirable forces caused by top plate motion.

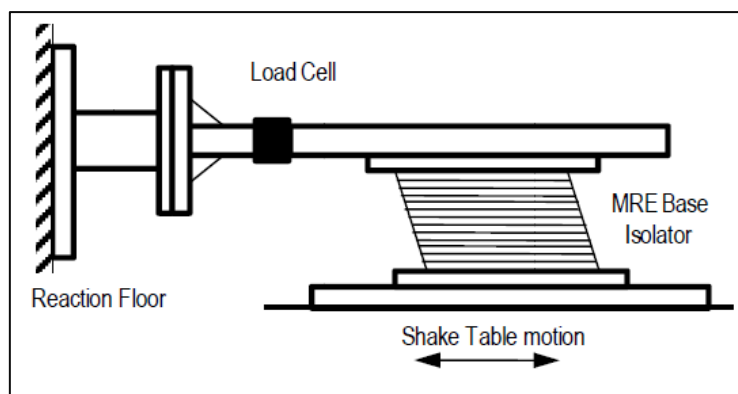


Figure 26: Experimental Setup for Stiffness Calculation

A specially designed load cell is used for calculating the forces exerted by the movement of the shake table. It is made up of a force sensor, a data collection controller, and controller modules that are tightly linked together using specialized circuit design and computer

programming. The maximum sensing capacity of the force sensor is 200N, with a sensitivity of 0.001N.

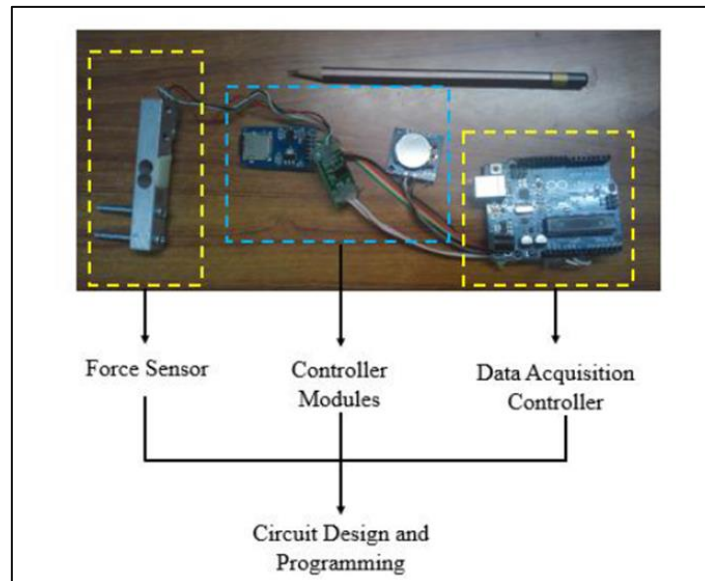


Figure 27: Components of Load Cell arrangement

The load cell is attached to the top plate on one end and to a fixed frame outside the table on the other. This setup allows the force exerted at the plate end (connected to the top plate) relative to the fixed end to be measured. A load cell is connected to a computer in which data can be saved for post-processing. Figure 35 depicts the load cell's constituent pieces. LVDT is used to calculate the displacement of base isolator. LVDT deals in microvolts. The volts can be calibrated against the displacement in mm. The resultant of the applied displacement and load obtained from the load cell provides stiffness. A DC power source energizes the magnetic coil for stiffness calculation under different values of current. A series of currents ranging from 0Amp-4Amp are given to the assembly during testing.

3.10 Mode Shapes

After manually calculating the Base Isolator's stiffness, a series of MATLAB experiments were carried out to determine its mode shapes at various stiffnesses of Base Isolator. While mode shapes do not represent an absolute value, they provide invaluable insight into the inherent deformability of the structure. The initial mode shape, also known as Mode Shape 1, depicts the fundamental mode of vibration and thus serves as a crucial representation of the structural response as a whole. Subsequently, modal analysis was utilized to determine the period and frequencies for both the isolated and fixed systems.

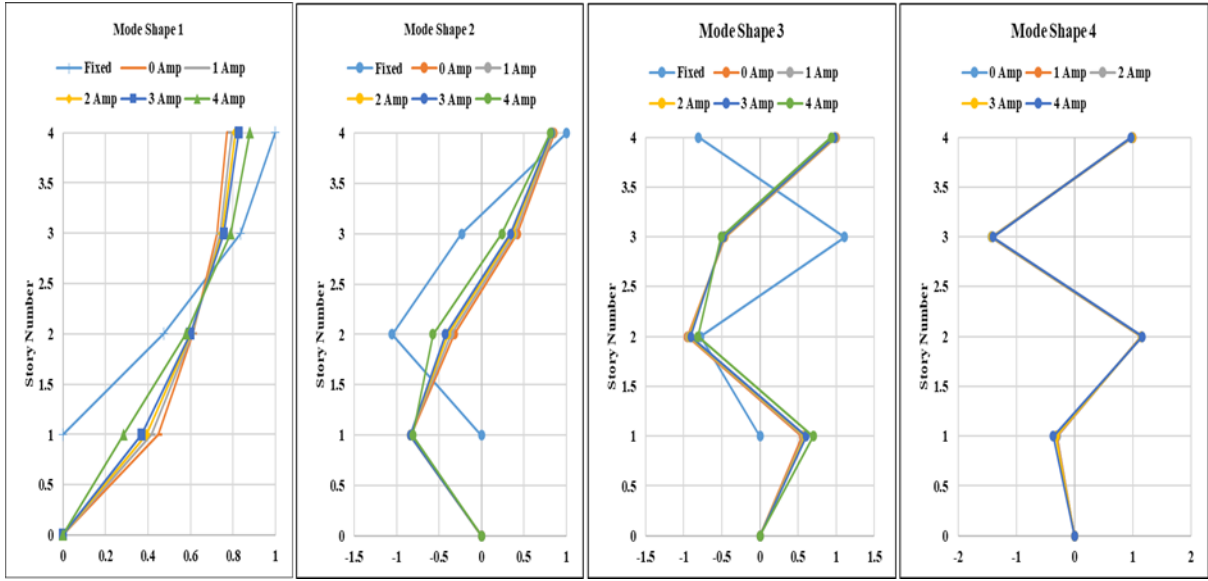


Figure 28: Mode Shapes of Fixed-base (Blue) and MRE isolated systems (others) at various current values

The provided Mode Shapes of the Fixed and Isolated Systems depict their respective dynamic behaviors visually normalized to the maximum value of the fixed system. Observations indicate that the isolated systems exhibit a larger base drift and a relatively smaller story drift. This differential response is a result of the base isolator's ability to mitigate dynamic forces and enhance its adaptability to differing conditions. Mode Shapes of Fixed and Isolated systems are shown in figure 36.

Significantly, the results provide an intriguing insight into the maximum displacement of the top story in the isolated case. This value is significantly lower than that of the fixed system, indicating that the base isolator is superior at mitigating the effects of dynamic loading. Time period and frequency of the fixed and Isolated systems are shown in the table:

Table 6: Frequency of Fixed base and Isolated System at various current values

Mode	Fixed	0 Amp	1 Amp	2 Amp	3 Amp	4 Amp
1	6.849	4.186	4.481593	4.683536	4.856218	5.432034
2	18.762	12.02	12.36253	12.64089	12.9139	14.14782
3	26.04	20.4	20.4779	20.54431	20.61451	21.02006
4		26.345	26.35419	26.36212	26.37047	26.41883

In conclusion, the MATLAB testing and subsequent analyses have yielded important insights regarding the mode structures, time periods, and dynamic responses of both isolated and fixed

systems. The displayed Mode Shapes and discernible differences in displacement patterns highlight the advantageous characteristics of the base isolator in mitigating the negative effects of dynamic forces compared to conventional fixed systems.

Table 7: Time Period of Fixed base and Isolated System at various current values

Mode	Fixed	0 Amp	1 Amp	2 Amp	3 Amp	4 Amp
1	0.146	0.238878	0.223135	0.213514	0.205922	0.184093
2	0.0533	0.083196	0.08089	0.079108	0.077436	0.070682
3	0.0384	0.049014	0.048833	0.048675	0.04851	0.047574
4		0.037958	0.037945	0.037933	0.037921	0.037852

3.11 Frame

A downscaled representation of a 3-storey Steel Frame has been employed as a prototype to investigate and analyze the structural behavior of the system. In this experimental setup, the Steel Frame serves as a surrogate for a full-scale structure, allowing for the observation of its response to various external stimuli. The modeling approach employed here conceptualizes the Steel Frame as a simplified three-degree-of-freedom (3 DOF) system. This representation involves considering lumped masses at distinct story levels and designating the columns as the primary components responsible for imparting stiffness to the frame.

It is noteworthy that the choice of this specific Steel Frame configuration was influenced by a preceding study involving base isolator. The initial frame utilized in that study exhibited a considerably reduced stiffness, which was congruent with the low stiffness characteristics of the base isolator material used in that study—predominantly attributable to the absence of iron particles. Consequently, a less stiff frame was deemed sufficient to effectively achieve the intended isolation objectives within that context.

However, the present study introduces a significant departure from this precedent. The utilization of a considerably stiffer isolator, as necessitated by the experimental requirements, mandates a reevaluation of the frame's stiffness characteristics. The shift in focus towards a more robust and stiffer isolator necessitates a corresponding adjustment in the stiffness properties of the frame to maintain compatibility and optimize the overall system response. Different frame and base isolator parameters of the previous study and present study are listed below.

Table 8: Initial and Modified frame properties after addition of stiffening components

Characteristics	Initial Frame	Modified Frame
Stiffness (N/mm)	4444	35555.6
Mass (Kg)	4.085	12.255
No. of Plates acting as Supporting Column	1	4
Base Isolator Stiffness(N/mm)	2200	9000



Figure 29: (a) Modified Steel Frame on Shake table (b) DC Supply for providing required values of current.

In summary, the scaled 3-storey Steel Frame stands as a critical component of the experimental setup, facilitating an in-depth examination of the structural dynamics under varying conditions. This choice was influenced by prior research involving base isolators, albeit with the recognition that the current study demands a distinctly stiffer frame to effectively accommodate the enhanced stiffness of the isolator. This cohesive integration of a more substantial and

responsive frame aligns with the study's objectives of comprehensively investigating the behavior of the coupled system in the context of base isolation.

Chapter 4: Results and Discussion

4.1 Experimental Setup

Dynamic testing was carried out on a reduced scale 3-DOF structure placed on a shake table. The shake table used is capable of supporting large vertical loads and providing a large number of lateral excitations. The steel structure is fitted with two isolators that help in the isolation process. Five LVDTs capable of determining the displacement were placed at all 3 storeys, base isolators and shake table. These LVDTs are first calibrated to make them fit for the purpose. Five accelerometers were also used to determine the acceleration response. These accelerometers are placed in the same manner as that of the LVDTs. Complete experimental setup is provided in figure 38.

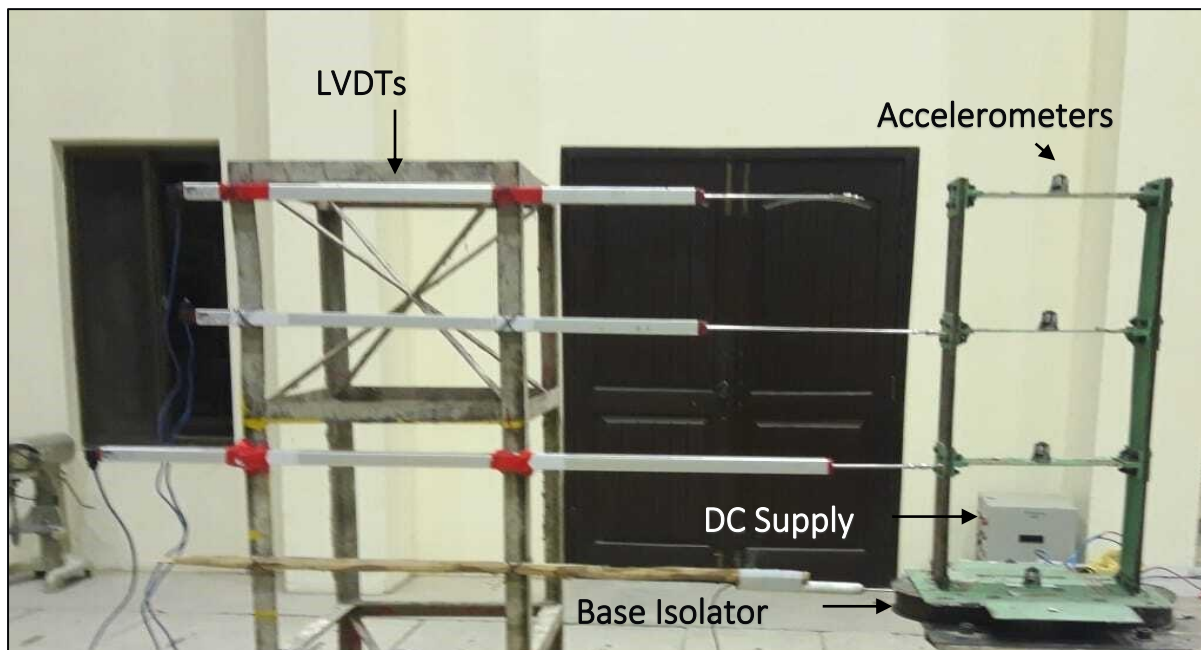


Figure 30: Experimental Setup for Dynamic Testing at various sinusoidal excitations

Base Isolators are fitted at the bottom of the frame. The wires wrapped around the non-magnetic coil have two ends. Both Isolators are connected in parallel and variable voltage depending upon the resistance of the isolators is provided. The voltage provides the necessary current for the study. This current is checked by an amperemeter and a relationship between current and voltage is determined as shown in figure 33.

A total of 45 sinusoidal excitations are tested for the shake table tests. Frequencies ranging from 0.5Hz, 1Hz and 1.5Hz are tested against the amplitudes of 5mm, 10mm and 15mm. All these combinations are tested for 0-4 Amperes.

Table 9: Parameters for different test cases

Test Parameter	Variation
Frequency	0.5Hz, 1Hz, 1.5H
Amplitude	5mm, 10mm, 15mm
Current	0A, 1A, 2A, 3A, 4A
Total no. of tests=45	

4.2 Effect of Amplitude

The recorded data includes the acceleration and displacement response for all storeys. The root mean square (RMS) values correspond to the structural vibrations of the building as a result of external loading. The experimental analysis conducted on the shake table frequently showed a reduction in displacement when the stiffness of a base isolator was increased. However, the reduction in response was not linear.

The optimal stiffness for reducing displacement at small amplitudes was found to be achieved by varying the current from 0 to 2 amperes. Nevertheless, contrary to expectations, an increase in displacement was seen instead of a reduction after 2Amp.

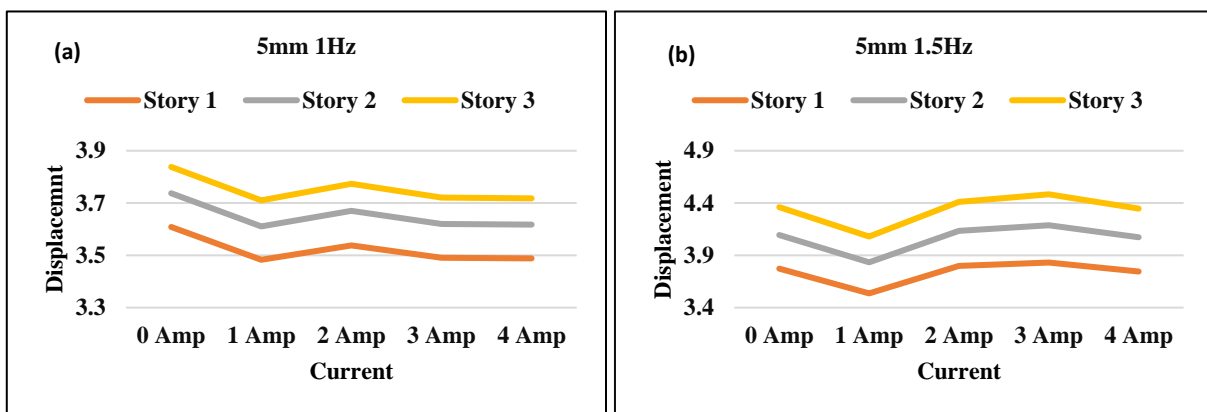


Figure 31:Effect of current in displacement reduction (a)5 mm 1Hz (b)5 mm 1.5Hz

The occurrence of this unforeseen outcome can be attributed to the fact that the stiffer isolators exhibited characteristics more akin to fixed systems rather than effectively isolating the structure. To clarify, when the stiffness is increased over a specific threshold, it results in a reduction in the isolator's capacity to properly isolate the structure. The largest reduction in

displacement for higher amplitudes, specifically 15mm and 10mm, was observed when the stiffness was at its maximum.

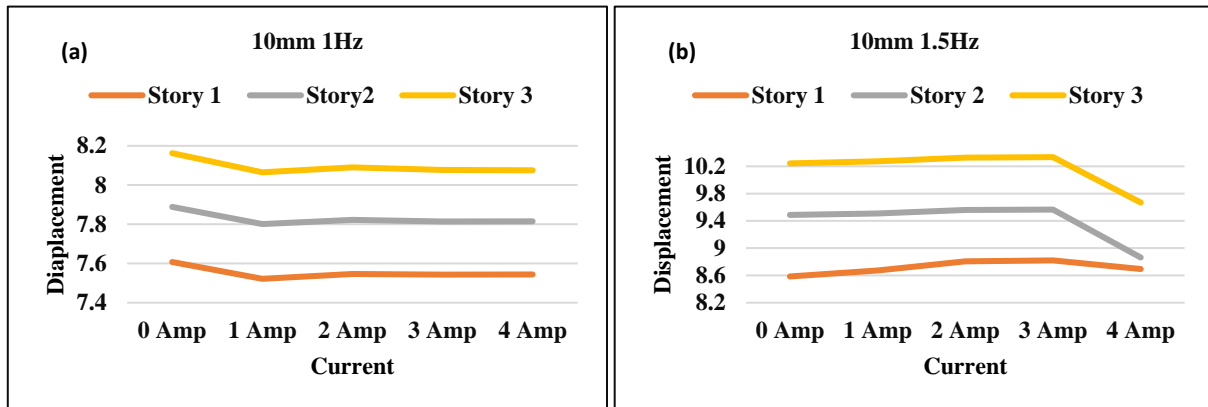


Figure 32: Effect of current in displacement reduction (a)10 mm 1Hz (b) 10 mm 1.5Hz

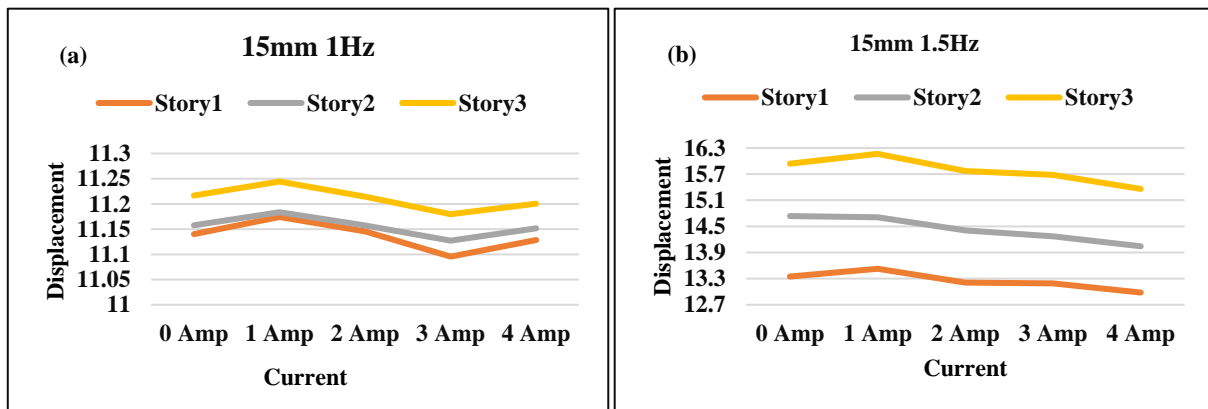


Figure 33: : Effect of current in displacement reduction (a)15mm 1Hz (b)15mm 1.5Hz

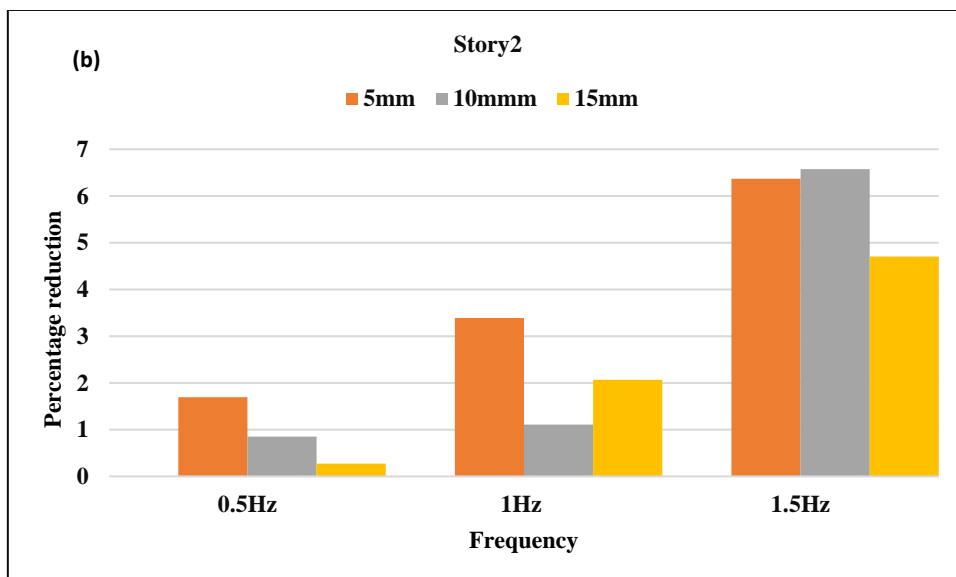
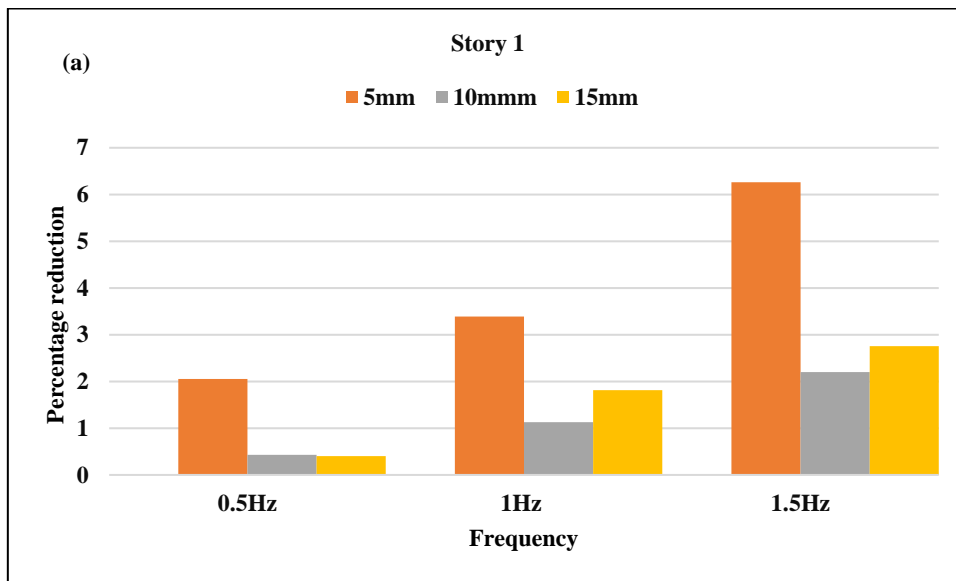
This phenomenon arises from the requirement of larger displacements, which in turn necessitate higher stiffness levels in order to properly counterbalance them. Previous research mostly focused on examining the impact of frequency and those investigations aimed to shift the frequency of the isolated system outside the seismic frequency band. This study additionally emphasizes the impact of amplitude on seismic isolation.

4.3 Effect of Frequency

The research findings emphasize a significant pattern in the decrease of overall displacement across different storeys of the structure. Significantly, the greatest significant reduction in displacement was recorded at an excitation frequency of 1.5Hz. This observation highlights the substantial impact of stimulation frequency on the structural response. When the excitation frequency closely matches the natural frequency of an isolated system, there is a significant possibility of experiencing severe displacement and even resonance. This study highlights the

observation that the most substantial decrease in structural response was observed when the excitation frequency approached the natural frequency of the system.

The ramifications of these studies have far-reaching significance for active systems that are endowed with variable stiffness. These systems exhibit the capability to adjust to a wide array of stimuli, hence increasing their adaptability in practical situations. Although displacement reduction was observed at low frequencies, it is most prominent in the vicinity of the system's native frequency. This observation highlights the crucial significance of resonance circumstances in shaping structural behavior.



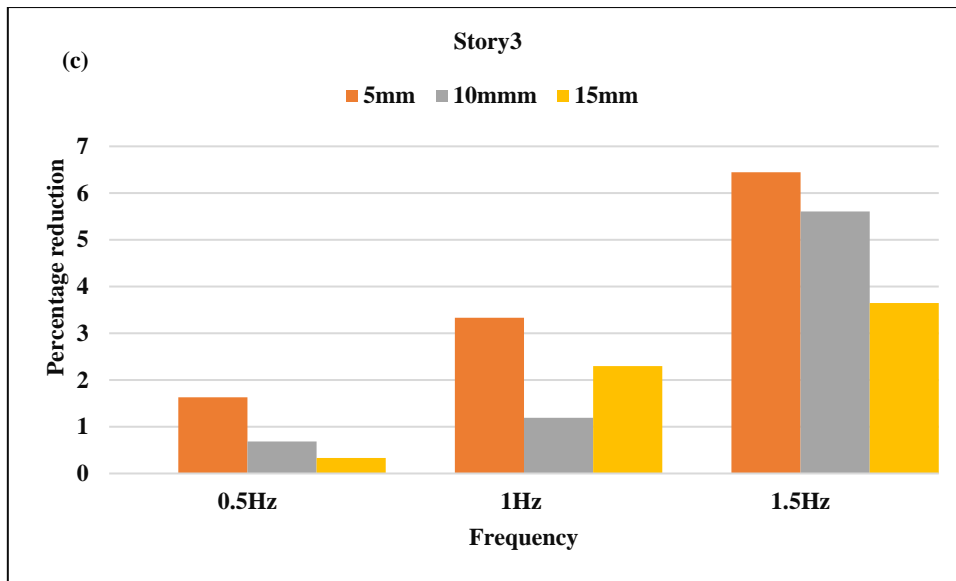


Figure 34: Effect of frequency in response reduction in (a) Story 1 (b) Story 2 (c) Story 3

The interaction between different stiffnesses and the extent of displacement reduction introduces an additional level of intricacy to the investigation. Various current settings result in different levels of reduction, highlighting the interconnectedness between system characteristics and the mitigation of responses. In order to enhance the effectiveness of the displacement reduction method, it is crucial to determine and utilize the most optimal current value. Through this approach, the system is able to efficiently mitigate the adverse consequences of resonance and its related displacement. Maximum reduction of 6 percent was seen for 1.5Hz highlighting the importance of loading frequency in dynamic analysis.

This study offers a complete analysis of the complex interrelationship between excitation frequency, natural frequency, and stiffness levels in dynamic systems. The observed relationship between the behavior of the system and the factors being examined highlights the possibility of customized solutions that can effectively utilize variable stiffness to reduce displacement.

4.4 Base Drift

The increased stiffness of the isolator played a crucial impact in reducing the displacement encountered by the isolation layer. The significant decrease in drift can be linked directly to the increased stiffness of the isolator. Nevertheless, it is crucial to acknowledge that this decrease was dependent on the particular current values that correlated with different degrees of stiffness. The correlation between stiffness and the reduction of drift was such that the most effective decrease in drift was achieved when the stiffness setting was at its maximum level.

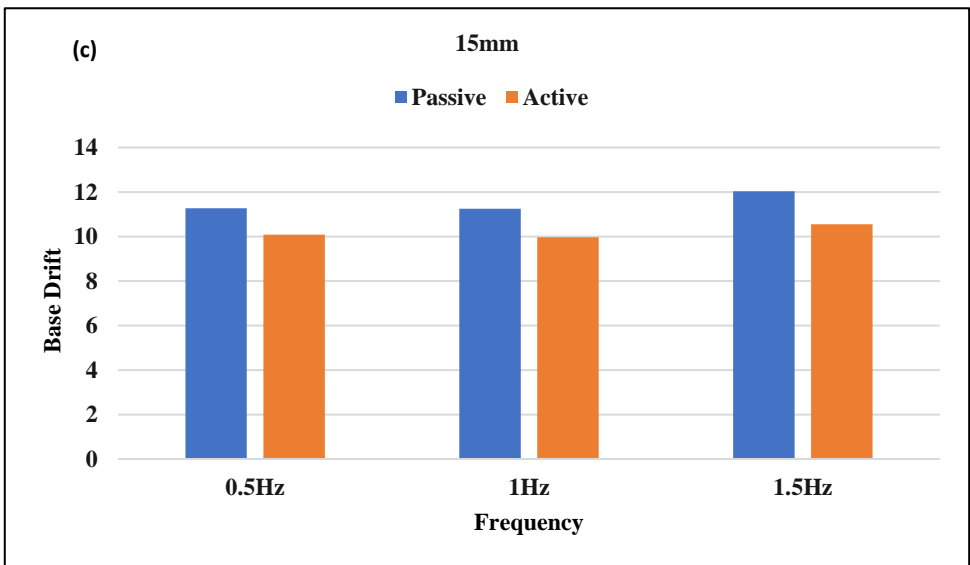
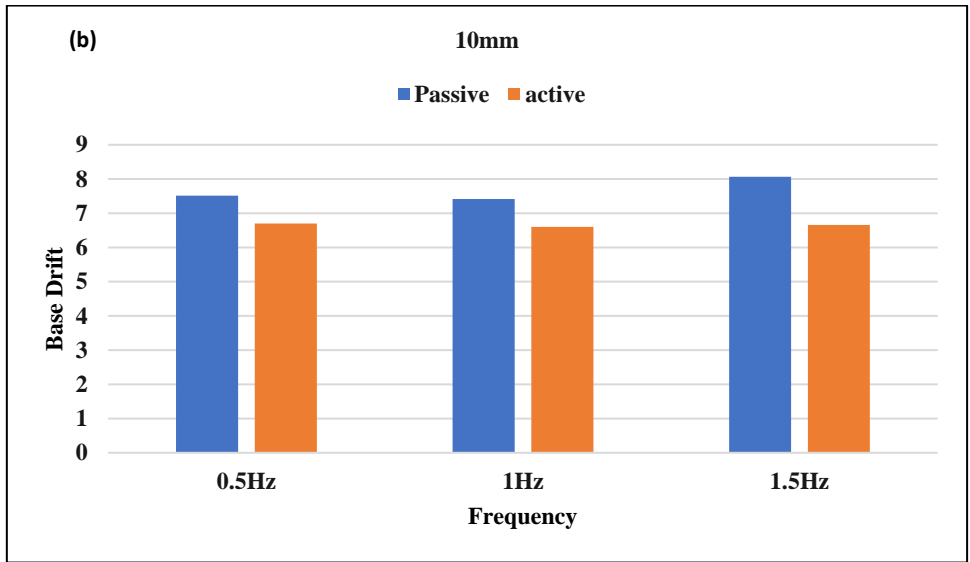
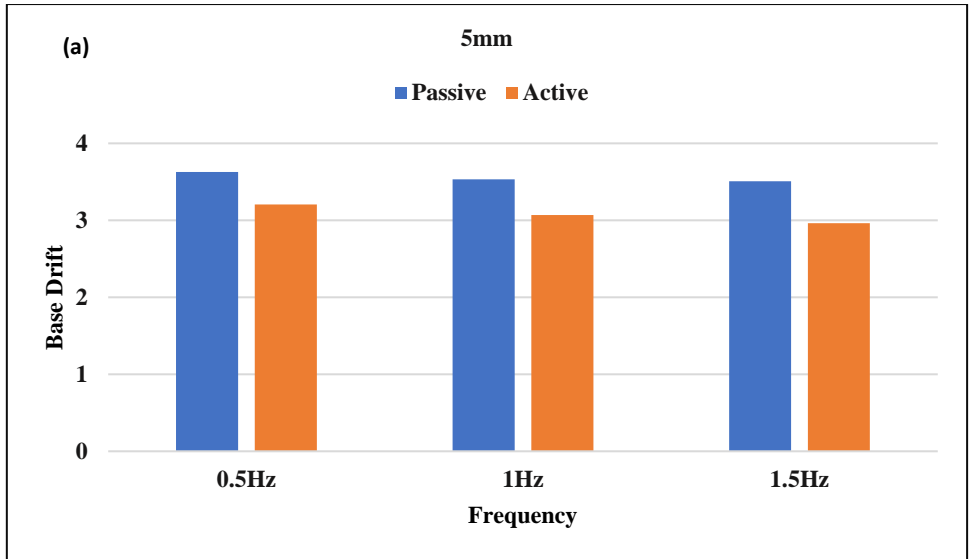


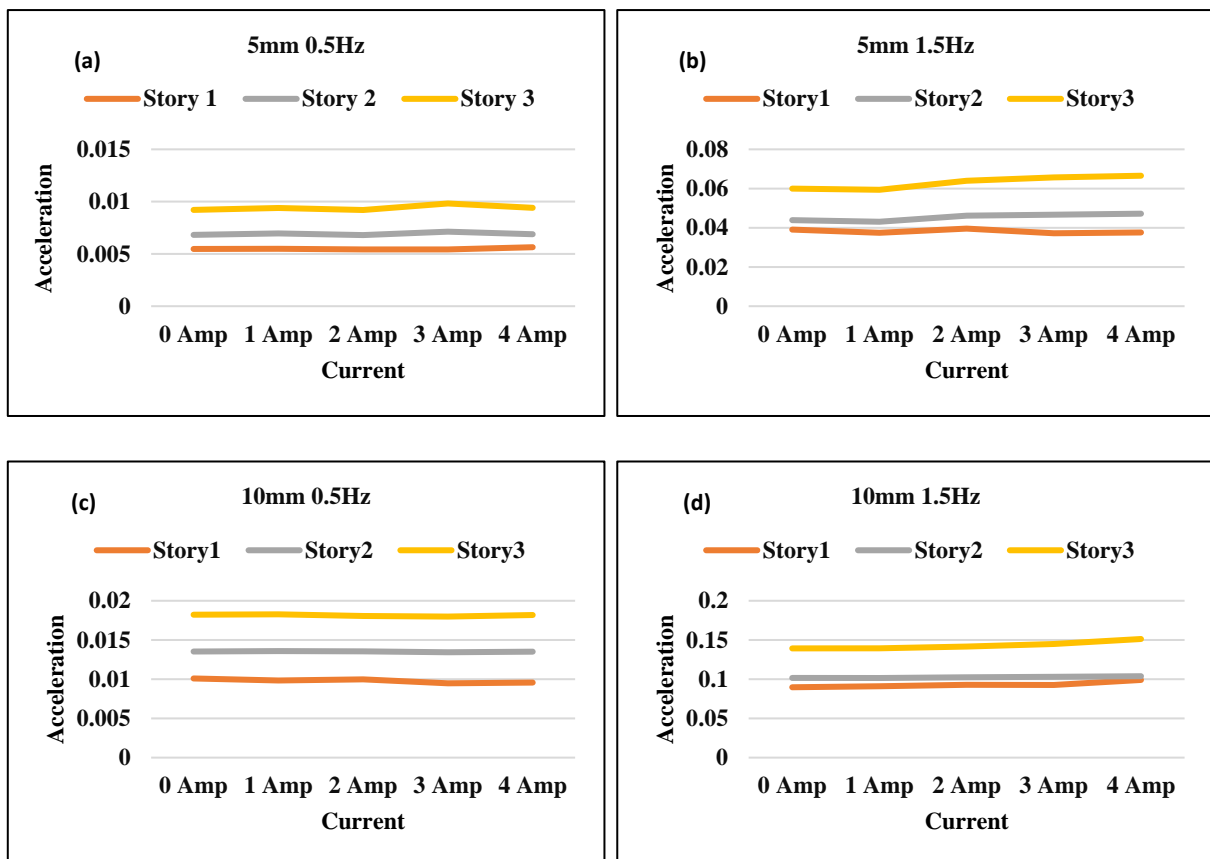
Figure 35: Base Drift reduction for (a) 5mm (b) 10mm (c) 15mm

Optimum current values were selected to control the base drift without compromising other key benefits of the isolators. This reduction in Base drift was observed at all combinations of frequencies and amplitudes.

4.5 Acceleration Response

The operational mechanism of Base Isolators is primarily based on the fundamental notion of mitigating acceleration amplification inside a structural system. The primary aim is to guarantee that the seismic forces or external vibrations exerted on the structure are neither amplified nor heightened by the isolator system. In contrast, the isolators are intricately designed with the purpose of absorbing and dispersing these forces, so efficiently isolating the structure from accelerations that have the potential to cause damage.

The empirical results obtained from the complete experimental investigation serve to validate and clarify this crucial principle. The findings, as illustrated in the accompanying typical graphs, clearly emphasize the lack of any substantial increase in acceleration. The presented graphs aptly depict the structural behavior and its corresponding response under different input situations.



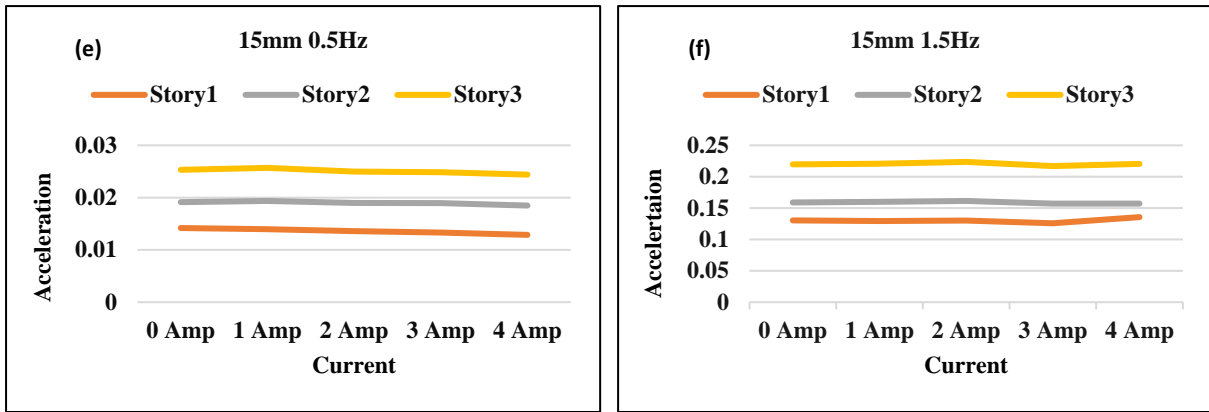


Figure 36: Acceleration response for (a) 5mm 0.5Hz (b) 5mm 1.5Hz (a) 10mm 0.5Hz (a) 10mm 0.5Hz (a) 15mm 0.5Hz (a) for 15mm 0.5Hz

The fundamental purpose of isolation is centered around minimizing story deviation inside a structural framework. The objective of this requirement is to reduce the lateral displacement encountered by various levels or stories of the structure during dynamic events, hence improving its stability and integrity. Nevertheless, a complex issue arises when contemplating the enhancement of isolator stiffness in the pursuit of this objective.

The intricate interplay between the stiffness of isolators and the magnitude of story drift gives rise to a complex equilibrium. Increasing the stiffness of isolators may potentially undermine the inherent benefit of decreased story drift that isolation aims to offer. This phenomenon occurs due to the potential danger of moving the system towards a fixed configuration, in which the structure exhibits less responsiveness to outside forces and diminished ability to accommodate lateral motions.

The concept of variable stiffness is a strategic solution that effectively manages the delicate balance at hand. By including the capability of modifying the stiffness of the isolator in accordance with dynamic circumstances, a state of optimal performance is attained. The isolator is able to optimize its behavior by employing an adjustable stiffness regime, which enables it to efficiently reduce story drift. This approach also ensures that the isolator avoids the drawbacks associated with a rigid system.

The empirical investigations conducted in this work provide evidence of the effectiveness of the variable stiffness paradigm. The isolation system, which incorporates dynamic stiffness modulation, demonstrated a notable capacity to finely adjust its response and effectively mitigate story drift. The achievement of optimization was clearly observed throughout a range of current values, with each value corresponding to a distinct stiffness setting.

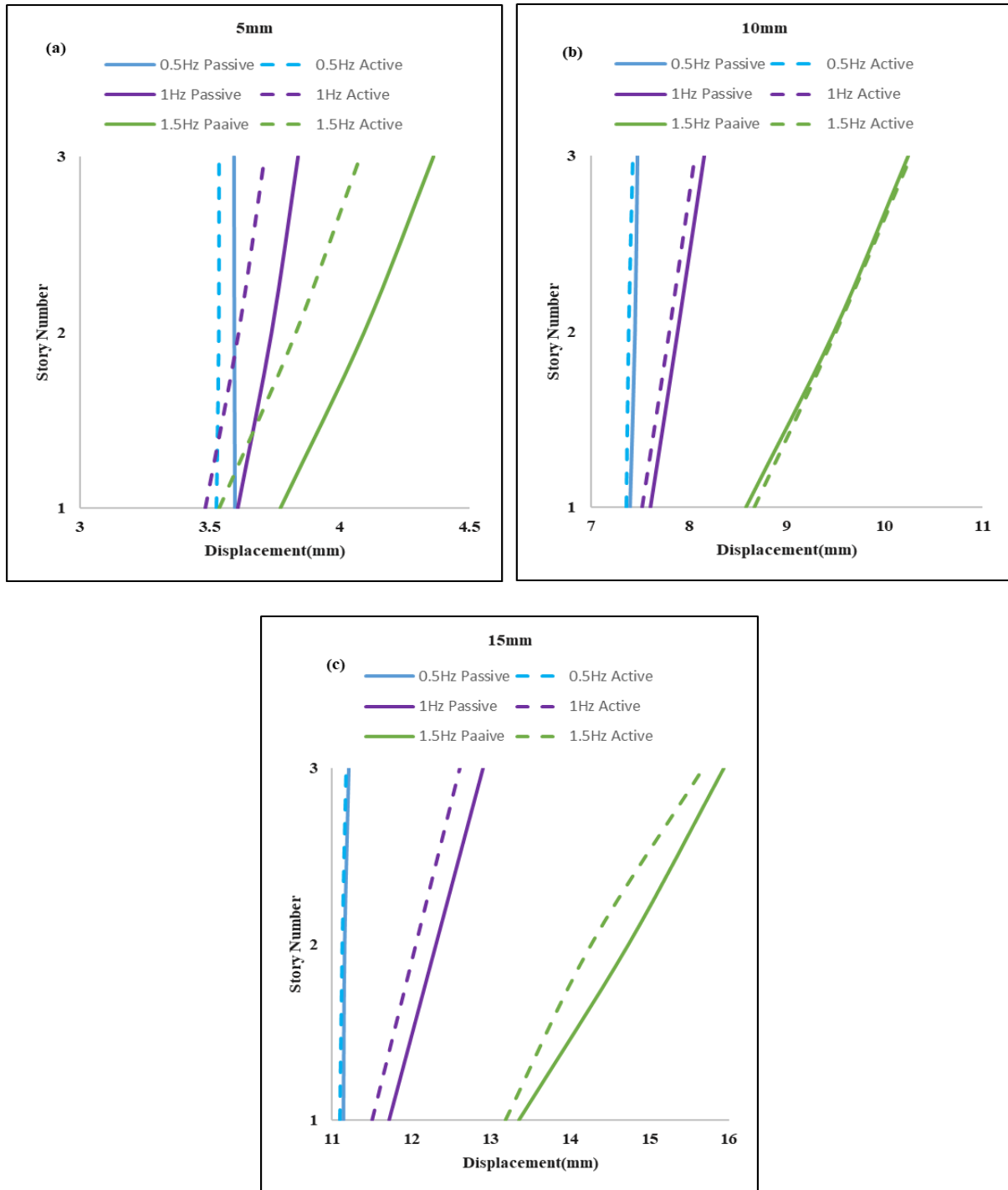


Figure 37: Story Drift reduction (a) 5mm (b) 10mm (c) 15mm

Optimum values of current for Story drift and Base Drift reduction are shown in table 10. As discussed earlier, for low amplitude the optimum reduction was achieved for 0-2 Amp. For 0.5Hz frequency for both 10mm and 15mm, the motion of the frame was rigid body motion. For such motion, a higher stiffness from 3A gave the best results. For all other base drifts maximum stiffness was optimum and for story drift at 10mm and 1Hz and 1.5Hz, low stiffness values were desirable. While for 15mm, high stiffness of 3A was desirable.

Table 10: Optimized Current Values for response reduction

	Story Drift			Base Drift		
	0.5Hz	1Hz	1.5Hz	0.5Hz	1Hz	15Hz
5mm	2(Amp)	1(Amp)	1(Amp)	2(Amp)	1(Amp)	1(Amp)
10mm	3(Amp)	1(Amp)	1(Amp)	3(Amp)	1(Amp)	3(Amp)
15mm	3(Amp)	3(Amp)	3(Amp)	3(Amp)	3(Amp)	3(Amp)

Chapter 5: Conclusion

The focus of the investigation was the design and evaluation of a variable stiffness base isolator for seismic applications. Multiple sinusoidal vibrations were applied to a framework, yielding the following results:

- The magnetic flux was optimized using Finite Element Magnetic Modelling (FEMM), achieving a flux of 0.12 Tesla with a 4 Amp current.
- Experiments on a shake table demonstrated that the stiffness can be increased by varying current in an active isolator at 4 Amps, stiffness increased from 9000N/mm to 22410N/mm, which corresponds to a Magnetic-Responsive (MR) effect increase of 149 percent.
- The natural time period of the isolated system increased from 0.146 seconds to 0.2388 seconds.
- The effectiveness of seismic isolation was dependent on frequency and amplitude. Lower stiffness (0-2 Amp range) was effective for 5 mm amplitude excitation, whereas higher stiffness was required for optimal response reduction during large amplitude excitations.
- At the system's inherent frequency of 1.5Hz and amplitudes of 5mm and 10mm, particularly at low current values, a notable reduction in displacement, about 6% for the second and third floors, was observed. This highlighted the importance of choosing an appropriate stiffness for effective isolation.
- There was no discernible increase in acceleration amplification as base isolator stiffness was increased.
- The implementation of a semi-active system decreased base drift without increasing acceleration or story drift specifications.

References

- [1] N. Lemarchand and J.-R. Grasso, "Interactions between earthquakes and volcano activity," *Geophysical Research Letters*, vol. 34, no. 24, 2007, doi: 10.1029/2007gl031438.
- [2] S. C. Pal *et al.*, "Earthquake hotspot and coldspot: Where, why and how?," *Geosystems and Geoenvironment*, vol. 2, no. 1, p. 100130, 2023/02/01/ 2023, doi: <https://doi.org/10.1016/j.geogeo.2022.100130>.
- [3] A. D. B. a. W. Bank, "Preliminary Damage and Needs Assessment," November 12, 2005.
- [4] A. K. Chopra and C. Chintanapakdee, "Comparing response of SDF systems to near-fault and far-fault earthquake motions in the context of spectral regions," *Earthquake Engineering & Structural Dynamics*, vol. 30, no. 12, pp. 1769-1789, 2001, doi: 10.1002/eqe.92.
- [5] B. F. Spencer and S. Nagarajaiah, "STATE OF THE ART OF STRUCTURAL CONTROL," *Journal of Structural Engineering-asce*, vol. 129, pp. 845-856, 2003.
- [6] J. Li, Y. Li, W. Li, and B. Samali, *Development of adaptive seismic isolators for ultimate seismic protection of civil structures*. 2013.
- [7] C. S. Tsai and H. H. Lee, "Applications of Viscoelastic Dampers to High-Rise Buildings," *Journal of Structural Engineering*, vol. 119, no. 4, pp. 1222-1233, 1993, doi: 10.1061/(asce)0733-9445(1993)119:4(1222).
- [8] G. M. Del Gobbo, A. Blakeborough, and M. S. Williams, "Improving total-building seismic performance using linear fluid viscous dampers," *Bulletin of Earthquake Engineering*, vol. 16, no. 9, pp. 4249-4272, 2018/09/01 2018, doi: 10.1007/s10518-018-0338-4.
- [9] W. H. Robinson, "Lead-rubber hysteretic bearings suitable for protecting structures during earthquakes," *Earthquake Engineering & Structural Dynamics*, vol. 10, no. 4, pp. 593-604, 1982, doi: 10.1002/eqe.4290100408.
- [10] Y. Shi, M. Kurata, and M. Nakashima, "Disorder and damage of base-isolated medical facilities when subjected to near-fault and long-period ground motions," *Earthquake Engineering & Structural Dynamics*, vol. 43, no. 11, pp. 1683-1701, 2014, doi: 10.1002/eqe.2417.
- [11] T.-T. Tran, T. T. H. Nguyen, and D. Kim, "Seismic incidence on base-isolated nuclear power plants considering uni- and bi-directional ground motions," *Journal of Structural Integrity and Maintenance*, vol. 3, pp. 86 - 94, 2018.

- [12] M. Ismail, J. Rodellar, and F. Ikhoulane, "An innovative isolation device for aseismic design," *Engineering Structures*, vol. 32, no. 4, pp. 1168-1183, 2010/04/01/ 2010, doi: <https://doi.org/10.1016/j.engstruct.2009.12.043>.
- [13] N. G. PATEL, "Study on a Base Isolation System," *International Journal of Innovative Science, Engineering & Technology*, vol. 1, no. 8, October 2014 2014.
- [14] B. Khan, M. Azeem, M. Usman, S. Farooq, and A. Hanif, "Effect of near and far Field Earthquakes on performance of various base isolation systems," 2019.
- [15] P. Pan, D. Zamfirescu, M. Nakashima, N. Nakayasu, and H. Kashiwa, "BASE-ISOLATION DESIGN PRACTICE IN JAPAN: INTRODUCTION TO THE POST-KOBE APPROACH," *Journal of Earthquake Engineering*, vol. 9, pp. 147 - 171, 2005.
- [16] U. R. Poojary and K. V. Gangadharan, "Integer and Fractional Order-Based Viscoelastic Constitutive Modeling to Predict the Frequency and Magnetic Field-Induced Properties of Magnetorheological Elastomer," *Journal of Vibration and Acoustics*, vol. 140, no. 4, 2018, doi: 10.1115/1.4039242.
- [17] H.-J. Jung, S.-H. Eem, D.-D. Jang, and J.-H. Koo, "Seismic Performance Analysis of A Smart Base-isolation System Considering Dynamics of MR Elastomers," *Journal of Intelligent Material Systems and Structures*, vol. 22, no. 13, pp. 1439-1450, 2011, doi: 10.1177/1045389x11414224.
- [18] M. Usman and H.-J. Jung, "Recent developments of magneto-rheological elastomers for civil engineering applications," 2015.
- [19] J.-H. Koo, D.-D. Jang, M. Usman, and H. J. Jung, "A feasibility study on smart base isolation systems using magneto-rheological elastomers," *Structural Engineering and Mechanics*, vol. 32, pp. 755-770, 2009.
- [20] N. Hoang, N. Zhang, and H. Du, "A dynamic absorber with a soft magnetorheological elastomer for powertrain vibration suppression," *Smart Materials and Structures*, vol. 18, no. 7, 2009, doi: 10.1088/0964-1726/18/7/074009.
- [21] G. Y. Zhou and Q. Wang, "Design of a smart piezoelectric actuator based on a magnetorheological elastomer," *Smart Materials and Structures*, vol. 14, no. 4, pp. 504-510, 2005, doi: 10.1088/0964-1726/14/4/007.
- [22] W. H. Li, X. Z. Zhang, and H. Du, "Magnetorheological Elastomers and Their Applications," in *Advances in Elastomers I: Blends and Interpenetrating Networks*, P. M. Visakh, S. Thomas, A. K. Chandra, and A. P. Mathew Eds. Berlin, Heidelberg: Springer Berlin Heidelberg, 2013, pp. 357-374.

- [23] D.-D. Jang, M. Usman, S.-H. Sung, Y.-j. Moon, and H.-j. Jung, "Feasibility Study of MR Elastomer-based Base Isolation System," 2008.
- [24] Y. Chae, J. M. Ricles, and R. Sause, "Large-Scale Experimental Studies of Structural Control Algorithms for Structures with Magnetorheological Dampers Using Real-Time Hybrid Simulation," *Journal of Structural Engineering*, vol. 139, no. 7, pp. 1215-1226, 2013, doi: 10.1061/(asce)st.1943-541x.0000691.
- [25] F. Mazza and A. Vulcano, "Effects of near-fault ground motions on the nonlinear dynamic response of base-isolated r.c. framed buildings," *Earthquake Engineering & Structural Dynamics*, vol. 41, 2012.
- [26] A. Boczkowska and S. F. Awietjan, "Microstructure and Properties of Magnetorheological Elastomers," *Advanced Elastomers-technology, Properties and Applications*, pp. 147-180, 09/12 2012, doi: 10.5772/50430.
- [27] X. Chen and J. Xiong, "Seismic resilient design with base isolation device using friction pendulum bearing and viscous damper," *Soil Dynamics and Earthquake Engineering*, vol. 153, p. 107073, 2022/02/01/ 2022, doi: <https://doi.org/10.1016/j.soildyn.2021.107073>.
- [28] M. Usman, S. H. Sung, D. D. Jang, H. J. Jung, and J. H. Koo, "Numerical investigation of smart base isolation system employing MR elastomer," *Journal of Physics: Conference Series*, vol. 149, no. 1, p. 012099, 2009/02/01 2009, doi: 10.1088/1742-6596/149/1/012099.
- [29] M. A. Tariq, M. Usman, S. H. Farooq, I. Ullah, and A. Hanif, "Investigation of the Structural Response of the MRE-Based MDOF Isolated Structure under Historic Near- and Far-Fault Earthquake Loadings," *Applied Sciences*, vol. 11, no. 6, 2021, doi: 10.3390/app11062876.
- [30] T.-T. Tran, T.-H. Nguyen, and D. Kim, "Seismic incidence on base-isolated nuclear power plants considering uni- and bi-directional ground motions," *Journal of Structural Integrity and Maintenance*, vol. 3, no. 2, pp. 86-94, 2018, doi: 10.1080/24705314.2018.1461547.
- [31] W. Fu, C. Zhang, M. Li, and C. Duan, "Experimental Investigation on Semi-Active Control of Base Isolation System Using Magnetorheological Dampers for Concrete Frame Structure," *Applied Sciences*, vol. 9, no. 18, 2019, doi: 10.3390/app9183866.
- [32] M. Tamim Tanwer, T. A. Kazi, and M. Desai, "A Study on Different Types of Base Isolation System over Fixed Based," in *Information and Communication Technology*

- for Intelligent Systems*, Singapore, S. C. Satapathy and A. Joshi, Eds., 2019// 2019: Springer Singapore, pp. 725-734.
- [33] A. Hameed, M.-S. Koo, T. D. Do, and J.-H. Jeong, "Effect of lead rubber bearing characteristics on the response of seismic-isolated bridges," *KSCE Journal of Civil Engineering*, vol. 12, no. 3, pp. 187-196, 2008, doi: 10.1007/s12205-008-0187-9.
- [34] C. Ma, D. Lu, and X. Du, "Seismic performance upgrading for underground structures by introducing sliding isolation bearings," *Tunnelling and Underground Space Technology*, vol. 74, pp. 1-9, 2018/04/01/ 2018, doi: <https://doi.org/10.1016/j.tust.2018.01.007>.
- [35] Y. Li and J. Li, "A Highly Adjustable Base Isolator Utilizing Magnetorheological Elastomer: Experimental Testing and Modeling," *Journal of Vibration and Acoustics*, vol. 137, no. 1, 2015, doi: 10.1115/1.4027626.
- [36] Y. K. Kim, J. H. Koo, K. S. Kim, and S. Kim, "Vibration isolation strategies using magneto-rheological elastomer for a miniature cryogenic cooler in space application," in *2010 IEEE/ASME International Conference on Advanced Intelligent Mechatronics*, 6-9 July 2010 2010, pp. 1203-1206, doi: 10.1109/AIM.2010.5695856.
- [37] P. D. Jadhao and S. M. Dumne, "Earthquake Performance of RC Buildings Using Elastomeric Base Isolation Controls," 2013.
- [38] J. Yang, S. S. Sun, S. W. Zhang, and W. H. Li, "Review of Structural Control Technologies Using Magnetorheological Elastomers," *Current Smart Materials*, vol. 4, no. 1, pp. 22-28, 2019, doi: 10.2174/2405465804666190326152207.
- [39] Y. Li, J. Li, W. Li, and B. Samali, "Development and characterization of a magnetorheological elastomer based adaptive seismic isolator," *Smart Materials and Structures*, vol. 22, no. 3, p. 035005, 2013/01/31 2013, doi: 10.1088/0964-1726/22/3/035005.
- [40] Y. Han, W. Hong, and L. E. Faidley, "Field-stiffening effect of magneto-rheological elastomers," *International Journal of Solids and Structures*, vol. 50, pp. 2281-2288, 2013.
- [41] Y. Li, J. Li, T. Tian, and W. Li, "A highly adjustable magnetorheological elastomer base isolator for applications of real-time adaptive control," *Smart Materials and Structures*, vol. 22, no. 9, 2013, doi: 10.1088/0964-1726/22/9/095020.
- [42] M. Bhandari, S. D. Bharti, and M. Shrimali, *BEHAVIOR OF BASE ISOLATED BUILDINGS SUBJECTED TO NEAR FIELD EARTHQUAKES*. 2017.

- [43] Y. Chae and J. M. Ricles, "Seismic Performance Enhancement of Base-Isolation Systems Using Semi-Active Damping Devices," 2012.
- [44] M. Lokander and B. Stenberg, "Performance of isotropic magnetorheological rubber materials," *Polymer Testing*, vol. 22, no. 3, pp. 245-251, 2003/05/01/ 2003, doi: [https://doi.org/10.1016/S0142-9418\(02\)00043-0](https://doi.org/10.1016/S0142-9418(02)00043-0).
- [45] P. Zając, J. Kaleta, D. Lewandowski, and A. Gasperowicz, "Isotropic magnetorheological elastomers with thermoplastic matrices: structure, damping properties and testing," *Smart Materials and Structures*, vol. 19, no. 4, 2010, doi: 10.1088/0964-1726/19/4/045014.
- [46] M. R. Jolly, J. D. Carlson, B. C. Muñoz, and T. A. Bullions, "The Magnetoviscoelastic Response of Elastomer Composites Consisting of Ferrous Particles Embedded in a Polymer Matrix," *Journal of Intelligent Material Systems and Structures*, vol. 7, pp. 613 - 622, 1996.
- [47] G. Y. Zhou, "Shear properties of a magnetorheological elastomer," *Smart Materials and Structures*, vol. 12, no. 1, pp. 139-146, 2003, doi: 10.1088/0964-1726/12/1/316.
- [48] L. Chen, X. L. Gong, and W. H. Li, "Microstructures and viscoelastic properties of anisotropic magnetorheological elastomers," *Smart Materials and Structures*, vol. 16, no. 6, pp. 2645-2650, 2007, doi: 10.1088/0964-1726/16/6/069.
- [49] L. Chen and X.-l. Gong, "Damping of magnetorheological elastomers," *Journal of Central South University of Technology*, vol. 15, no. 1, pp. 271-274, 2008/09/01 2008, doi: 10.1007/s11771-008-0361-8.
- [50] S. U. Khayam, M. Usman, M. A. Umer, and A. Rafique, "Development and characterization of a novel hybrid magnetorheological elastomer incorporating micro and nano size iron fillers," *Materials & Design*, vol. 192, p. 108748, 2020/07/01/ 2020, doi: <https://doi.org/10.1016/j.matdes.2020.108748>.
- [51] J. D. Carlson and M. R. Jolly, "MR fluid, foam and elastomer devices," *Mechatronics*, vol. 10, no. 4, pp. 555-569, 2000/06/01/ 2000, doi: [https://doi.org/10.1016/S0957-4158\(99\)00064-1](https://doi.org/10.1016/S0957-4158(99)00064-1).
- [52] S. Hegde, K. Kiran, and K. V. Gangadharan, "A novel approach to investigate effect of magnetic field on dynamic properties of natural rubber based isotropic thick magnetorheological elastomers in shear mode," *Journal of Central South University*, vol. 22, no. 7, pp. 2612-2619, 2015/07/01 2015, doi: 10.1007/s11771-015-2791-4.

- [53] Z.-d. Xu, Y. Liao, T. Ge, and C. Xu, "Experimental and Theoretical Study of Viscoelastic Dampers with Different Matrix Rubbers," *Journal of Engineering Mechanics-asce*, vol. 142, p. 04016051, 2016.
- [54] L. Meunier, G. Chagnon, D. Favier, L. Orgéas, and P. Vacher, "Mechanical experimental characterisation and numerical modelling of an unfilled silicone rubber," *Polymer Testing*, vol. 27, pp. 765-777, 2008.
- [55] L. Ge, X. Gong, Y. Fan, and S. Xuan, "Preparation and mechanical properties of the magnetorheological elastomer based on natural rubber/rosin glycerin hybrid matrix," *Smart Materials and Structures*, vol. 22, no. 11, 2013, doi: 10.1088/0964-1726/22/11/115029.
- [56] C. Castro and B. Mitchell, "Nanoparticles from Mechanical Attrition," *Synthesis, Functionalization and Surface Treatment of Nanoparticles*, 01/01 2002.
- [57] Y. Umehara *et al.*, "Railway Actuator Made of Magnetic Elastomers and Driven by a Magnetic Field," *Polymers*, vol. 10, 2018.
- [58] M. A. Osman and A. Atallah, "Effect of the particle size on the viscoelastic properties of filled polyethylene," *Polymer*, vol. 47, no. 7, pp. 2357-2368, 2006/03/22/ 2006, doi: <https://doi.org/10.1016/j.polymer.2006.01.085>.
- [59] M. Lokander and B. Stenberg, "Improving the magnetorheological effect in isotropic magnetorheological rubber materials," *Polymer Testing*, vol. 22, no. 6, pp. 677-680, 2003/09/01/ 2003, doi: [https://doi.org/10.1016/S0142-9418\(02\)00175-7](https://doi.org/10.1016/S0142-9418(02)00175-7).